

1 Dear editor and reviewer,

2 Thank you for your positive comments and very important recommendations to improve our  
3 manuscript. We have carefully modified the manuscript based on your suggestions and provide a  
4 response to each comment. Reviewer comments are given in black, and responses are given in  
5 blue. Below we provide a marked-up manuscript version showing the changes based on your  
6 comments. The main modifications to the manuscript are as follows:

- 7 1. The descriptions about the SVR SD retrieval algorithm were added in *Section 3.2 "Processing*  
8 *flow overview"* according to your suggestions (Page 11)
- 9 2. The equations for analysis metric were added in *Appendix* (Page 21)
- 10 3. We revised the order "extremely significant increase, significant increase, non-significant  
11 change, extremely significant decrease, and significant decrease" to "extremely significant  
12 decrease, significant decrease, non-significant change, significant increase, and extremely  
13 significant increase" in Table 5, Fig. 8 and Fig. 11 according to your suggestions.

14  
15 Please see below the detailed responses (in blue color).

16  
17 **REVIEWER 1#**

18 I reviewed the paper titled, tc-2019-33-AC1-supplement.pdf, which was a revision of the  
19 paper after the previous reviewer pointed out a calculation error.

20 In this study, SWE and snow depth data over North America are developed over a long period  
21 of record, 1992-2016, to evaluate spatial and temporal trends in snow mass and snow cover  
22 duration during that time. The study uses a SVR method which combines passive microwave  
23 data with other variables to estimate snow depth. They compute SWE using seasonally  
24 varying density estimates developed for different snow classes. They find overall decreasing  
25 trends in snow mass during the study period, particularly after 2002, though results vary  
26 regionally and at different rates seasonally.

27 The paper needs a thorough English language review. The developed data and analysis are  
28 interesting and important, but at times it is difficult to understand exactly what was done. In  
29 particular, the variation rate analyses are unclear. I suggest adding equation for this metric,  
30 and maybe all of them, to make it obvious what was done. Beyond that, my main feedback is  
31 to provide additional high-level details about the SVR method. The way the paper is written it  
32 is mandatory that the reader refers to Xiao et al. 2018 in order to understand the process.  
33 Enough detail should be given here that the reader has a high-level understanding of the SVR  
34 algorithm and the process steps involved.

35  
36 Response: Thank you very much for your review of our manuscript. We appreciate your positive  
37 comments and very useful suggestions for improving the manuscript. We made modification  
38 according to your suggestion. The point-by-point revisions are as follows.

39  
40  
41 Specific comments:

42 Page 6, Line 29: SSM/I is listed twice.

1 Response: Thanks. We have changed “SSMIS (Special Sensor Microwave Imager), SSM/I  
2 (Special Sensor Microwave Imager Sounder)” to “SSM/I (Special Sensor Microwave Imager),  
3 SSMIS (Special Sensor Microwave Imager Sounder)” in Page 2, lines 27-28.

4  
5 Page 8, line 11: “SVR” hasn’t been defined in article yet.

6 Response: We have added the description of SVR, support vector regression in Page 4, line 8.

7  
8 Page 9, lines 15-18: If only 9000 stations are valid, why were 17000 used? How were they  
9 selected? Does the map (figure 1) show all the stations, or just the ones used in this study? I would  
10 recommend only showing the stations used.

11 Response: Thank you very much. This sentence “Data at approximately 30000 meteorological  
12 stations were recorded of which 9000 typically are valid” have been revised to “Data at  
13 approximately 30000 meteorological stations were recorded of which more than 9000 station are  
14 currently obtainable” in Page 5, line 11. Stations with observation dates between 1992 and 2016  
15 were selected in this work. Due to the observation time in some station of this historical dataset  
16 are very short, e.g. 1 year, 2 year, even less than one year. Hence, the station used in our work  
17 (about 17000) is greater than the number of stations currently obtainable. Figure 1 show the  
18 stations finally selected.

19  
20 Page 11, line 4: “SD”, which actually is SWE” Can you explain what this means?

21 Response: The sentence ““SD”, which actually is, is one of the thirteen parameters provided” was  
22 changed to “SWE, which is labeled as SD in this dataset, is one of the thirteen parameters  
23 provided” in page 6, line 28 .

24  
25 Page 11, line 24: List of parameters (DS, A, T, G, L, D) are used in sentence but not defined until  
26 later. They should be defined when first used. I would recommend revising the sentence to  
27 something like “The snow retrieval process uses various parameters to yield snow depth (Xiao et  
28 al. 2018).

29 Response: Than you very much. We changed “The snow retrieval process uses DS and other  
30 parameters (A, T, G, L, D ...) to yield snow parameters (e.g. SD, Eq. 1) (Xiao et al., 2018)” to  
31 “The snow retrieval process uses various parameters to yield snow parameters (e.g. SD, Eq. 1)  
32 (Xiao et al., 2018)” in page 7, lines 18-19

33  
34 Page 13, lines 13-23: I’m not sure what is meant by layers. Do you mean layers within the  
35 snowpack? Or are you referring to observations of snow at low, medium and high depths?

36 Response: These three layers mean the low, medium and high snow depths. We changed “Firstly,  
37 the numbers of sample in the three layers, layer1 ( $0 \leq SD < 50$ ), layer2 ( $50 \leq SD < 100$ ) and layer3  
38 ( $SD \geq 100$ ), should be concretely quantified” to “Firstly, the numbers of sample in the three layers  
39 that split up by snow depth should be concretely quantified, i.e. layer1 ( $0 \leq SD < 50$ ; low depth),  
40 layer2 ( $50 \leq SD < 100$ ; medium depth ) and layer3 ( $SD \geq 100$ ; high depth)” in page 9, lines 18-20

41  
42 Page 13, line 29: the part of the sentence, “or medium-to-deep” doesn’t seem like it fits. Should  
43 this be removed?

44 Response: Thanks, we removed “or medium-to-depth” in this sentence in page 10, line 1.

1  
2  
3  
4  
5  
6  
7  
8  
9  
10  
11  
12  
13  
14  
15  
16  
17  
18  
19  
20  
21  
22  
23  
24  
25  
26  
27  
28  
29  
30  
31  
32  
33  
34  
35  
36  
37  
38  
39  
40  
41  
42

Page 14, equation 2: units of density are wrong if you want SWE in mm. Should use a density ratio (snow density/water density) to keep units consistent. (since density of water is 1 g/cm<sup>3</sup>, values will be the same)

Response: Thanks. We have revised the original formula to “  $SWE(mm) = SD(cm) \times \rho_{snow}(g/cm^3)/\rho_{water}(g/cm^3) \times 10$ ” in page 10, Eq. 2

Page 14, line 21. Why do you have “(decrease)” here?

Response: Thank you. We have removed “(decrease)” in this sentence in page 10 line 23.

Page 16, line 24: I think “shadow” should be “shallow”

Response: We changed “shadow” to “shallow” in page 12 line 23.

Page 17, line 26: Switch the order of “extremely significant decrease” and “significant decrease” so that the 5 grades are listed in order from largest increase to decrease. Same with Figure 8 and Table 5.

Response: Thanks. We have revised the original order to “extremely significant decrease, significant decrease, non-significant change, significant increase, and extremely significant increase” in this sentence (page 13 lines 24-26) and the description in Table 5, Fig. 8 and Fig. 11.

Page 18, line 25-26: Can you provide the equation for this metric: “Seasonal average SD was defined as the cumulative SD divided by the days in one snow cover season”? It’s not clear to me what is being computed.

Response: Thanks. This sentences “Seasonal average SD was defined as the cumulative SD divided by the days in one snow cover season” can be described by the following formula.

$$SD_{average} = \frac{\sum_{i=1}^n SD_i}{n} \tag{1}$$

$n$  is the number of days in one snow cover season,  $i$  is  $i$ th day in one snow cover season. This formula have been added in Appendix.

Page 20, lines 9-11: Maximum snow mass is occurring later in the year? This is in contrast to most recent literature that is finding max SWE occurring earlier.

Response: Thank you very much. We have searched and consulted plenty of literature about snow mass or snow water equivalent. Perhaps because of the limited research data available to us, we have not found a study on the occurrence time of maximum snow mass on the hemisphere scale. More research is on the change trend of the snow mass or the maximum SWE. Our finding is consistent with other research conclusions, and it is found that the snow mass or maximum SWE exhibits a decreasing trend in the long-term sequence (Section 4.2). As described in Section 4.2 and Section 3.3, snow mass is calculated by SWE multiplied by snow cover area; SWE is derived from snow depth and snow density. One reason may be due to the temporal and spatial differences in snow depth and snow density distribution, the snow mass finally generated will also vary in different study areas, resulting in different occurrence time for maximum snow mass. Therefore, this conclusions on the hemisphere scale may be contrary to the findings of the small study area or regions. Moreover, with the increase in temperature, precipitation may be another reason that

1 affects the downward trend of the maximum snow mass in March. Kumar et al. (2012) quantified  
2 the impacts of more extreme precipitation regimes (MEPR) on the maximum seasonal snow water  
3 equivalent and found that MEPR potentially alleviate the maximum seasonal snow water  
4 equivalent decrease trend. It should be noted that in our future work, we will further study the  
5 impact of extreme precipitation conditions and or climatic factors on the trend of snow mass  
6 change in the northern hemisphere.

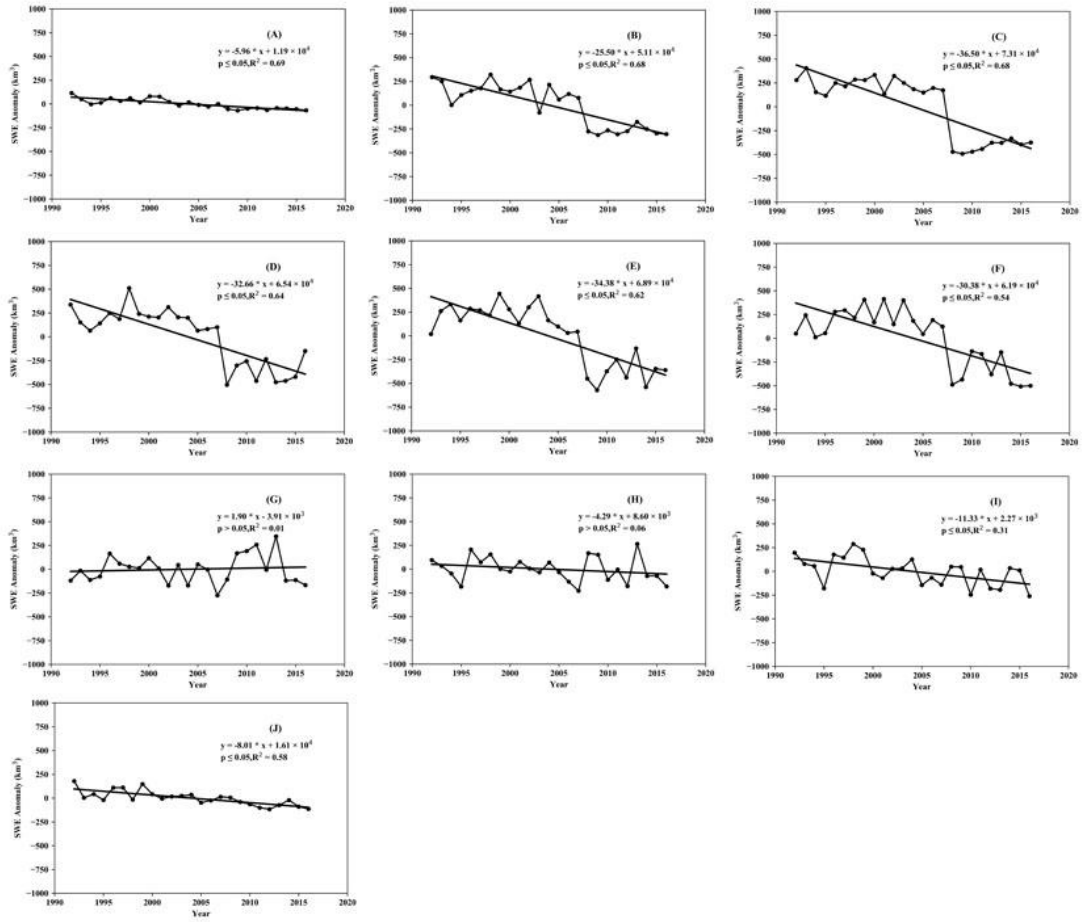
7 We added this sentence “This finding need to be further analyzed in the future work by correlation  
8 with climatic factors, such as precipitation effects (Kumar et al., 2012)” in page 16 lines 5-6.

9  
10 Kumar, M., Wang, R., & Link, T.E. (2012). Effects of more extreme precipitation regimes on  
11 maximum seasonal snow water equivalent. *Geophysical Research Letters*, 39

12  
13 Page 20, line 27 (and Table 7): it seems strange that February average snow mass rate decreases  
14 significantly, while March increases slightly. Is this snow that accumulated during each month or  
15 average snow mass at the time? Can you add text stating why you think that is? It would also be  
16 nice to see the data and how the months compare. You could create a figure like Figure 10,  
17 showing the time series for all the months in different colors.

18 Response: Thank you. The statement “An increasing trend appears in March with a rate of  
19 approximately 1.9068 km<sup>3</sup> yr.<sup>-1</sup> ( $P > 0.05$ ), however, relatively large decrement in fall and winter  
20 are unable to partially be offset by the increment of March.” have been revised to “However, there  
21 are no significant trends in March and April with large interannual variations (Table 7)” in page 16  
22 lines 20-23.

23 The monthly average snow mass index used in here is the average of the snow mass in each day of  
24 this month. So this index only describe snow cover information during this month. Figures 1  
25 exhibits the anomalies of monthly average snow mass (from September to June) from 1992  
26 through 2016 with respect to the 1992–2016 average across the Northern Hemisphere. Table 7 and  
27 Figures 1-F showed an significant decrease trends in February average snow mass with  $R^2 = 0.54$ ;  
28 while Mach average snow mass is no significant trends with large interannual variation,  $R^2 = 0.009$ .  
29 In general, monthly average snow mass shows decrease from September to June except March and  
30 April, no trends with large interannual variability in March and April.



1  
2  
3  
4  
5  
6  
7  
8

Figures. 1. The anomalies of monthly average snow mass (from September to June) from 1992 through 2016 with respect to the 1992–2016 average across the Northern Hemisphere. (A) September. (B) October. (C) November. (D) December. (E) January. (F) February. (G) March. (H) April. (I) May. (J) June.

# Spatiotemporal variation of snow depth in the Northern Hemisphere from 1992 to 2016

Xiongxin Xiao<sup>1,2</sup>, Tingjun Zhang<sup>1,4</sup>, Xinyue Zhong<sup>3</sup>, Xiaodong Li<sup>1</sup>, Yuxing Li<sup>1</sup>

<sup>1</sup>Key Laboratory of Western China's Environmental Systems (Ministry of Education), College of Earth and Environment Sciences, Lanzhou University, Lanzhou 730000, China

<sup>2</sup>School of Remote Sensing and Information Engineering, Wuhan University, Wuhan 430079, China

<sup>3</sup>Key Laboratory of Remote Sensing of Gansu Province, Cold and Arid Regions Environmental and Engineering Research Institute, Chinese Academy of Sciences, Lanzhou 730000, China

<sup>4</sup>University Corporation for Polar Research, Beijing 100875, China.

*Correspondence to:* Tingjun Zhang (tjzhang@lzu.edu.cn)

**Abstract:** Snow cover is an effective best indicator of climate change due to its effect on regional and global surface energy, ~~water balance~~, hydrology, climate, and ecosystem function. We developed a long term Northern Hemisphere daily snow depth and snow water equivalent product (NHSnow) by the application of the support vector regression (SVR) snow depth retrieval algorithm to historical passive microwave sensors from 1992 to 2016. The accuracies of the snow depth product were evaluated against observed snow depth at meteorological stations along with the other two snow cover products (GlobSnow and ERA-Interim/Land) across the Northern Hemisphere. The evaluation results showed that NHSnow performs generally well with relatively high accuracy. Further analysis were performed across the Northern Hemisphere during 1992-2016, which used snow depth, snow mass and, snow cover days as indexes. Analysis showed annual average snow mass has a significant declining trends ( $\sim 19.72 \text{ km}^3 \text{ yr}^{-1}$ , 13% reduction). Although spatial variation pattern of snow depth and snow cover days exhibited slight regional differences, it generally reveals a decreasing trend over most of the Northern Hemisphere. Our work provides evidence that rapid changes in snow depth and snow water equivalent are occurring beginning at the turn of the 21<sup>st</sup> century with dramatic, surface-based warming.

## 1. Introduction

Seasonal snow cover is an important component of the climate system and global water cycle that stores large amounts of freshwater and play major impacts on the surface energy budget, climatology and water management (Immerzeel et al., 2010;Zhang, 2005;Robinson and Frei, 2000;Tedesco et al.,

1 2014). On account of the high albedo and low heat conductivity properties of snow, snow cover may  
2 directly modulate the land surface energy balance (Flanner et al., 2011), influence on soil thermal  
3 regime (Zhang et al., 1996;Zhang, 2005), and indirectly affect atmospheric circulation (Cohen et al.,  
4 2012;Zhang et al., 2004;Li et al., 2018). Most jurisdictions in the Northern Hemisphere rely on natural  
5 water storage provided by snowpack (Differbaugh et al., 2013;Barnett et al., 2005), supplying water for  
6 domestic and industrial use (Sturm, 2015;Qin et al., 2006). Accurate estimation of and reliable  
7 information on snow cover spatial and temporal change at regional and global scales is very critical for  
8 climate change monitoring, model evaluation and water source management (Brown and Frei,  
9 2007;Flanner et al., 2011).

10 Snow depth (SD) is most commonly measured using in situ observations. Given the sparseness of  
11 measurements, it is not possible to fully capture spatial variability of snow cover. Although the in situ  
12 observation method is accurate, it is unrealistic in mountain regions and low population zones because  
13 it is labor, material and financial resource intensive. Remote sensing is the most effective and powerful  
14 way of obtaining information of snow cover over larger areas (Foster et al., 2011). Optical remote  
15 sensing is capable of observing large areas of snow; however, it is unable to observe the Earth's surface  
16 under cloudy conditions (Foster et al., 2011;Che et al., 2016;Dai et al., 2017). However, microwave  
17 remote sensing has this potential and is an attractive alternative to optical remote sensing under all  
18 weather conditions and round the clock. It can also be used to estimate SD and snow water equivalent  
19 (SWE) due to the interaction with snowpack by providing dual polarization data at different  
20 frequencies (Chang et al., 1987;Che et al., 2008;Takala et al., 2011).

21 Snow cover products derived from passive microwave (PM) data have been widely applied to  
22 investigate regional and global climate change, and validate hydrological and climate models (Brown et  
23 al., 2010;Brown and Robinson, 2011;Dai et al., 2017). Progress in satellite data acquisition, as well as  
24 SD/SWE retrieval algorithm development, have led to a global improvement in snow monitoring (Qin  
25 et al., 2006;Snauffer et al., 2016). The PM brightness temperature of the SMMR (Scanning  
26 Multichannel Microwave Radiometer), SSM/I (Special Sensor Microwave Imager), AMSR-E  
27 (Advanced Microwave Scanning Radiometer for Earth Observing System), AMSR2 (Advanced  
28 Microwave Scanning Radiometer 2 on the Global Change Observation Mission – Water), [SSM/I](#)  
29 (Special Sensor Microwave Imager), [SSMIS](#) (Special Sensor Microwave Imager Sounder) and,  
30 FY-3B/C (Fengyun-3 satellite B/C) are available and several algorithms have been developed to

1 estimate SD and SWE using PM brightness temperature data (Chang et al., 1987;Dai et al., 2012;Xiao  
2 et al., 2018;Pulliainen, 2006;Takala et al., 2011;Che et al., 2008;Foster et al., 1997).

3 Most retrieval algorithms operate on the principle that the difference in brightness temperature  
4 between 18 and 37 GHz reflects the quantity of SD and SWE (Chang et al., 1987). Over and  
5 underestimated trends are prevalent in these linear SD and SWE retrieval algorithms (Gan et al., 2013)  
6 for which there are two possible and reasonable explanations. One is that vegetation overlaying snow  
7 attenuates its microwave scatter signal and results in underestimating SD and SWE from PM data (Che  
8 et al., 2016;Vander Jagt et al., 2013). To reduce the effect of tree canopy, a forest fraction was  
9 introduced into retrieval algorithm developed to estimate SD and SWE (Foster et al., 1997;Che et al.,  
10 2008), or the retrieval algorithm was constructed based on particular land cover types (Goïta et al.,  
11 2003;Che et al., 2016;Derksen et al., 2005;Foster et al., 2009). The other explanation is that the  
12 relationship between snow properties (SD or SWE) and the PM brightness temperature is non-linear.  
13 Newer approaches (e.g. artificial neural networks, support vector regression, decision tree) have  
14 emerged using data-mining and have been explored to retrieve SD and SWE that are intended to  
15 replace traditional linear methods (Gharaei-Manesh et al., 2016;Tedesco et al., 2004;Liang et al.,  
16 2015;Forman et al., 2013;Xue and Forman, 2015). However, there are remain some limitations for  
17 these retrieval algorithms due to the diversity of land cover types and the spatiotemporal heterogeneity  
18 of snow physical properties.

19 Numerous studies have reported the changes in snow cover extent (SCE) at regional and  
20 hemispheric scales (Rupp et al., 2013;Dai et al., 2017;Derksen and Brown, 2012;Brown and Robinson,  
21 2011;Huang et al., 2016). Huang et al. (2017) reported the impact of climate and elevation on snow  
22 cover variation in Tibetan Plateau, including SWE, snow cover area and, snow cover days. Hori et al.  
23 (2017) developed a 38-year Northern Hemisphere daily snow cover extent product and analyzed  
24 seasonal Northern Hemisphere snow cover extent variation trends. In this study, SD was selected as  
25 basis for analyzing spatiotemporal change of snow cover. SD provides an additional dimension to snow  
26 cover characteristics. Barrett et al. (2015) explored intra-seasonal variability in springtime Northern  
27 Hemisphere daily SD change by the phase of the Madden–Julian oscillation. Wegmann et al. (2017)  
28 compared four long-term reanalysis datasets with Russian SD observation data. However, this study  
29 only focused on snowfall season (October and November) and snowmelt season (April). SD change  
30 trends have also been analyzed at regional scales (Ye et al., 1998;Dyer and Mote, 2006). Several studies

1 quantified the spatial and temporal changes consistency of SWE or snow mass derived from satellite  
2 data (Mudryk et al., 2015) but these studies have focused on the limited dimension of snow cover  
3 variation. Dyer and Mote (2006) used a gridded dataset to study regional and temporal variability of  
4 SD trends across North America from 1960-2000 –and the characteristic of seasonal snow extent and  
5 snow mass in South America form 1979 to 2006 was described and reported (Foster et al., 2009).

6 There are, however, very limited data (station data, satellite data or otherwise) that can provide  
7 both SD and SWE on a hemispheric scale. This paper describes the approach to develop a consistent  
8 25-year of daily SD and SWE of Northern Hemisphere utilized multi-source data. The primary  
9 objective of this study is to develop 25 years (1992-2016) hemispherical SD and SWE product  
10 (hereafter referred to as the NHSnow) with a 25 km spatial resolution using [support vector regression](#)  
11 (SVR) SD retrieval algorithm. This paper will address the following questions: 1) How consistent are  
12 NHSnow and other sourced snow cover datasets with the in situ SD observation? 2) What is the  
13 spatiotemporal variability of snow cover in the Northern Hemisphere from 1992-2016? Meanwhile, it  
14 is extremely challenging to make extensive quantitative validation of SD and SWE estimates.

15 This paper is organized in five sections, as follows. Section 2 describes the data sets used in this  
16 study. The methods of data preprocessing and snow cover products generation were provided in  
17 Section 3. Next, we describe NHSnow validation against in-situ snow observation records, exhibit the  
18 variability of snow cover in the Northern Hemisphere and discuss the potential effect factors for the  
19 variation results utilized NHSnow data (Section 4). Finally, section 5 summarizes the work of this  
20 paper.

## 21 **2 Datasets**

### 22 **2.1 Passive microwave data**

23 Because cloud often appear in the snow cover region or condition, during the winter season often  
24 conceals snowfall possibility, here is particularly advantageous using passive microwave remote  
25 sensing. SSM/I and SSMIS is PM radiometer onboard United States Defense Meteorological Satellites  
26 Program (DMSP) satellite (available from the National Snow and Ice Data Center,  
27 <http://nsidc.org/data/NSIDC-0032>). The SSM/I (F11 and F13) dataset from this platform, as well as  
28 SSMIS (F17), present with the equal-area scale earth grid (EASE-Grid) format and 25 km spatial

1 resolution (Brodzik and Knowles, 2002;Armstrong, 2008;Wentz, 2013;Armstrong and Brodzik, 1995)  
2 (Table 1). The snow cover area and SD derived from SSM/I (F11) and SSM/I (F13) data have high  
3 consistency rendering the calibration between these two sensors for snow cover area and SD  
4 unnecessary (Dai et al., 2015). To minimize the melt-water effect to some extent, which can change the  
5 microwave emissivity of snow, only descending orbit (nighttime) passive microwave data were used  
6 (Foster et al., 2009).

## 7 **2.2 Ground-based data**

8 Ground SD observation are used to construct and verify the SD retrieval model in this study from  
9 two sources of daily SD observation. The first is the Global Surface Summary of the Day (GSOD)  
10 dataset provided by National Oceanic and Atmospheric Administration (NOAA)  
11 (<https://data.noaa.gov/dataset/dataset/global-surface-summary-of-the-day-gsod>). This online dataset,  
12 which began in 1929, is derived from the Integrated Surface Hourly (ISH) dataset (Xu et al., 2016).  
13 There are fourteen daily elements in GSOD dataset, including SD measured at 0.1 inch. The missing of  
14 SD or reported 0 on the day would be marked 999.9. Data at approximately 30000 meteorological  
15 stations were recorded of which more than 9000 station are typically obtainable. In our study period  
16 and area, more than 17 000 meteorological station were selected with records from 1991 and a location  
17 far from large water bodies.

18 To supplement data from stations that were not reporting during the study periods, ground-based  
19 measurements of daily SD were gathered from an additional 635 Chinese meteorological stations  
20 available at the National Meteorological Information of China Meteorological Administration (Xiao et al.  
21 al., 2018;Zhong, 2014). These daily SD records begun in 1957 include SD (unit, cm), observation time,  
22 and geographical location information available (<http://data.cma.cn/en>).

## 23 **2.3 Topographic and land cover data**

24 We also used topography as an auxiliary information to estimate SD (Xiao et al., 2018). Elevation  
25 was available from ETOPO1 at a resolution of 1 arc-minute (Amante, 2009) available at  
26 (<http://www.ngdc.noaa.gov/mgg/global/>). To match the resolution of the PM brightness temperature  
27 data with 25 km spatial resolution, we resampled the ETOPO1 to 25 km resolution (Fig. 1).

28 To increase the accuracy of SD estimates for different land cover types, we both used MODIS land

1 cover (MCD12Q1 V051) from 2001 to 2013 (Friedl and Sulla-Menashe, 2011;Friedl et al., 2010) and  
2 Advanced Very High Resolution Radiometer (AVHRR) Global Land Cover classification generated by  
3 the University of Maryland Department of Geography. The MCD12Q1 International  
4 Geosphere-Biosphere Program (IGBP) classification scheme divides land surface into 17 types, which  
5 were reclassified into five classes according to Xiao et al (2018) study.

6 AVHRR imagery was acquired between 1981-1994 from the NOAA-15 satellite (Hansen et al.,  
7 2000) and were categorized into fourteen land cover classes at 1 km resolution. These data allowed us  
8 to adjust the proposed snow-depth retrieval algorithm by reclassifying the fourteen native land cover  
9 classes into five classes (water, forest, shrub, prairie and, bare-land) at 25 km spatial resolution (Table  
10 A.). MCD12Q1 is available at site <https://earthdata.nasa.gov/>, while AVHRR land cover data is  
11 available from <http://www.landcover.org/data/landcover/>.

## 12 **2.4 Satellite snow cover datasets**

13 Two kinds of snow cover datasets were utilized based on two criteria: covering the Northern  
14 Hemisphere and long-term availability. We selected GlobSnow and ERA-Interim/Land which are  
15 widely used in global and regional climate change studies (Snauffer et al., 2016;Hancock et al.,  
16 2013;Mudryk et al., 2015). These datasets were used to compare with the NHSnow SD product.

17 In November 2013, the European Space Agency (ESA) released the GlobSnow Version 2.0 SWE  
18 and Snow Extent (SE) data for the Northern Hemisphere (Takala et al., 2011;Pulliainen, 2006). These  
19 data include all non-mountainous areas in the Northern Hemisphere and are available online  
20 (<http://www.globsnow.info/>). Processing includes data assimilation based on combining satellite PM  
21 remote sensing data (SMMR, SSM/I and SSMIS), spanning December 1979 to May 2016, with  
22 ground-based observation data in a data assimilation scheme to derive SWE. GlobSnow Version 2.0  
23 (hereinafter referred as GlobSnow) provides three kinds of temporal aggregation level products with  
24 25 km spatial resolution: daily, weekly and monthly. This dataset covers all land surface areas in a  
25 band between 35° N ~ 85° N excluding mountainous regions, glaciers and Greenland. To convert  
26 between SD and SWE using GlobSnow, the snow density is held constant at 0.24 g/cm<sup>3</sup> (Sturm et al.,  
27 2010;Hancock et al., 2013;Che et al., 2016).

28 ERA-Interim/Land (Balsamo et al., 2015) is a global land-surface reanalysis product with data  
29 from January 1979 to December 2010 based on ERA-Interim meteorological forcing. It is produced by

1 a land-surface model simulation using the Hydrology Tiled ECMWF Scheme of Surface Exchange  
2 over Land (HTESSEL), with meteorological forcing from ERA-Interim. Dutra et al. (2010) described  
3 the snow scheme and demonstrated the verification using field experiments. [SWE, which is labeled as](#)  
4 [SD in this dataset](#), is one of the thirteen parameters provided. We should convert SWE to SD using the  
5 associated snow density data. These two datasets are available online  
6 (<http://apps.ecmwf.int/datasets/data/interim-land/type=an/>). To maximum the proximity to the  
7 descending orbit time of passive microwave sensor, the data with analysis type at 6 o'clock were used  
8 in this study, and the spatial resolution of these data is 0.125 degree.

## 9 **2.5 Snow classification data**

10 In order to accurately estimate SWE, snow classification data were used to convert SD into SWE.  
11 Global Seasonal Snow Classification System was defined by Sturm et al. (1995) based on snow  
12 physical properties (SD, thermal conductivity, snow density snow layers, degree of wetting, etc.), and  
13 seasonal snow cover. Snow cover were categorized into six snow classes (tundra, taiga, alpine,  
14 maritime, prairie, and ephemeral) plus water and ice fields (Figure 2). Snow classification data can be  
15 accessed from the National Center for Atmospheric Research (NCAR)/Earth Observing Laboratory  
16 (EOL) (<https://data.eol.ucar.edu/dataset/6808>). The snow classification dataset was developed and  
17 tested for the Northern Hemisphere at 0.5-degree spatial resolution(Sturm et al., 1995).

## 18 **3 Methods**

### 19 **3.1 Theoretical basis**

20 Snow distribution is affected by various factors, but not limited to, vegetation (Che et al.,  
21 2016;Vander Jagt et al., 2013), soil and air temperature (Forman and Reichle, 2015;Grippa et al.,  
22 2004;Dai et al., 2017), topography and wind (Smith and Bookhagen, 2016). [The snow retrieval process](#)  
23 [uses various parameters to yield snow parameters](#) (e.g. SD, Eq. 1) (Xiao et al., 2018).

$$[S] = g(A, T, G, L, DS, D \dots) + \varepsilon \quad (1)$$

24 where  $g(\cdot)$  denotes the retrieval function. DS is the digital signal from remote sensing sensor (PM,  
25 active microwave, visible spectral remote sensing etc.), A is the atmosphere (wind speed, air  
26 temperature, humidity, precipitation etc.), T is the topography (latitude, longitude, elevation, terrain

1 slope, aspect etc.), L is the location (latitude, longitude), G is the ground (ground surface temperature,  
2 vegetation type etc.), S is the snow properties (snow grain size, density, reflectance, SD, SWE etc.), D  
3 is the day of year and  $\varepsilon$  is the residual error or uncertainty that describes the relationship between  
4 sensor signal and measured snow properties.

5 The SVR SD retrieval algorithm also follows the snow retrieval process (Eq. 1). We utilized ten  
6 parameters were as input parameters, including PM brightness temperature (19 GHz, 37 GHz, 85 GHz,  
7 or 91 GHz) with vertical and horizontal polarizations, geophysical location (latitude and longitude),  
8 elevation and, the measured SD. The output parameter is the estimated SD. Apart from above factors,  
9 the SVR SD retrieval algorithm also considers other influence factors, including wet snow, land cover  
10 types and day of year (Xiao et al., 2018) to improve the accuracy of estimated SD. Day of year have  
11 been converted into three snow cover stages, which mean indirectly considering snow properties  
12 evolution.

### 13 **3.2 Processing flow overview**

14 The SVR SD retrieval algorithm first proposed by Xiao et al. (2018), which indirectly considers  
15 seasonal variation and vegetation influence in the evolution of snow properties, was used to estimate  
16 SD. In Eurasia, it was found that the SVR SD retrieval algorithm performs much superior with reduced  
17 uncertainties compared based upon the correlation coefficient (R), mean absolute error (MAE), and  
18 root mean squared error in Xiao et al. (2018) study. It should be noted that this study used daily  
19 observation in the Northern Hemisphere with exception of July and August. ~~Here, we provide more~~  
20 ~~detailed but different descriptions for the SVR SD retrieval algorithm in several steps (Fig. 3).~~ We  
21 shortly described the SVR SD retrieval algorithm involved six steps (see Fig. 3): step 1 is data  
22 preprocessing about meteorological station SD observations and PM brightness temperature data;  
23 Before estimating SD using PM data, it is necessary to identify snow cover and dry snow by a set of  
24 criteria in step 2; To segregate the land cover effect on snow cover distribution (step 3) and snow  
25 properties evolution effect (step 4), SD retrieval model were established on different land cover types  
26 (forest, shrub, prairie, bare-land) and snow cover stages (snow cover accumulation, stabilization and  
27 ablation stage); in step 5, we chose SVR as retrieval function (Eq. 1) with specific kernel functions and  
28 parameters; step 6 is constructing a set of SD retrieval models trained by the suitable size and quality  
29 training samples. The more detailed descriptions of these ~~other~~ steps can refer to the Xiao et al paper

(Xiao et al., 2018) ~~not repeated here~~. Here, we provide more detailed but different descriptions for the SVR SD retrieval algorithm in several steps (cf. Fig. 3).

Step 3. Due to the study period pre-dates MODIS data, we used AVHRR land cover as supplement data. MODIS and AVHRR land cover were reclassified into four classes (forest, prairie, shrub and bare-land) which were bases of constructing SD retrieval sub-model. Table A (in appendix) describes the reclassification scheme of AVHRR land cover is described. MODIS land cover reclassification schemes were documented in Xiao et al. (2018). Because of the relative stability of land cover change, MODIS land cover in 2013 was used for each year during 2013–2016. Similarly, MODIS land cover in 2001 was used in each year during 1998–2001, and AVHRR land cover data were used for 6 years (1992–1997).

Step 6.1 Construction of a subcontinental model. It needs to be stressed that the snow properties in the Eurasia (EU) and North America (NA) exhibit noticed discrepancy especially in snow density. (Zhong et al., 2014; Bilello, 1984). One study pointed out that mean snow density in the former Soviet Union ( $0.21 \sim 0.31 \text{ g/cm}^3$ ) was lower than the data from NA ( $0.24 \sim 0.31 \text{ g/cm}^3$ ) (Bilello, 1984), and also Zhong et al. (2014) explained the possible reasons which resulting in the diversity of snow density in EU and NA. Based on this, we separately constructed the SD retrieval models for EU and NA.

Step 6.2 Training dataset selection is the process of removing redundant features from spatial data. The accuracy of estimated SD primarily depends on training data quality, which also demonstrate the significance of the selection rule of training samples (Xiao et al., 2018). Inputting more data than needed in the training dataset to train SD retrieval model, may lead to overfitting and an estimated SD with high error. In this study, we collected an extremely large number of daily SD records over 25 years, necessitating a optimized selection rule to avoid data information redundancy.

The selection rule proposed in previous research (Xiao et al., 2018) was modified and then it was divided into two steps in here. Firstly, the numbers of sample in the three layers that split up by snow depth should be concretely quantified, i.e. layer1 ( $0 \leq \text{SD} < 50$ ; low snow), layer2 ( $50 \leq \text{SD} < 100$ ; medium depth) and layer3 ( $\text{SD} \geq 100$ ; high depth). To avoid an inflated training sample in layer2 and layer3, we set a threshold (3 000) determined by several tests (not shown). A threshold (12000) for layer1 was adopted following Xiao et al. (2018). Table 2 described the section of training sample for each layer in detail. After that, the quality of training sample in each layers determined by stratified random sampling is the second step. Stratification was performed in 1 cm SD intervals. Note that, all

1 the selection operations in here were randomly performed.

2 Step 7. Through above steps, the daily estimated SD data in the Northern Hemisphere from  
3 January 1992 to December 2016 (excluding July and August) were obtained. Owing to the nature of  
4 radiometer observations, NHSnow products are only reliable in areas with seasonal dry snow cover.  
5 Areas with sporadic wet or thin snow are not reliably detected and areas marked as snow-free may  
6 include areas with wet snow. If one pixel is detected as snow cover by the detection decision tree  
7 (Grody and Basist, 1996), but is likely to be shallow-~~or medium to deep~~ snow with an estimated value  
8 of equal or less than 1 cm, the SD value is set as 5 cm (Che et al., 2016; Wang et al., 2008) (Fig. 4).

9 Step 8. In this study, Greenland and Iceland are excluded from the generation and analysis of  
10 NHSnow (NH\_SD, NH\_SWE) products due to their complex coastal topography and the difficulty in  
11 discriminating snow from ice (Fig. 4) (Brown et al., 2010). Missing data and zero-data gaps occur in  
12 the process of generating daily SD gridded products. Therefore, the following filters were applied.  
13 Daily estimated SD was averaged with a sliding 7-day window to reduce noise and compensate for  
14 missing data in the daily time series. For example, the SD estimate for 4 January is an average of the  
15 assimilated scheme output for 1 to 7 January (Takala et al., 2011; Che et al., 2016). When finished, the  
16 sliding SD method generated daily SD products for the entire Northern Hemisphere (NH\_SD; Fig. 4).

### 17 3.3 Estimation of SWE

18 SWE contains more useful information for hydrologists than SD because it represents the amount  
19 of liquid water in the snowpack available to the ecosystem as the snow melts. One way to estimate  
20 SWE uses SD and snow density ( $\rho_{snow}$ ) as described in Eq. 2. Northern Hemisphere SWE products  
21 were generated in this study using snow density that converts SD to SWE. (Eq. 2, Fig. 3 and 4, Step 9).

$$22 \quad SWE(mm) = SD(cm) \times \rho_{snow}(g/cm^3) / \rho_{water}(g/cm^3) \times 10 \quad (2)$$

23 At present, the primary problem is to obtain relatively accurate snow density. In this study,  
24 dynamical calculation methods were adopted to estimate snow density. Two methods are usually used  
25 to convert SD to SWE. The first uses a fixed value, 0.24 g/cm<sup>3</sup> (or other value), without spatiotemporal  
26 variation (Che et al., 2016; Takala et al., 2011). The second uses a temporally static by spatially variable  
27 mask of snow density to estimate SWE and are used to generate current AMSR-E SWE products  
28 (Tedesco and Narvekar, 2010). Since the snowpack are usually rather unstable, it is awfully  
unreasonable to set the snow density in the whole snow season to a constant. Observations show that

1 | snow density does evolve and tends to increase—(decrease) throughout the snow season (from  
2 | September to June) (Dai et al., 2012;Sturm et al., 1995). Here, daily snow density is obtained following  
3 | Sturm et al.(2010) (Eq. 3).They used daily SD, day of the year (DOY), and the snow climate class (SC)  
4 | to produce snowpack bulk density estimates. In this method, knowledge of SC is used to capture field  
5 | environment variables (air temperature, initial density) that have a considerable effect on snow density  
6 | evolution.

$$\rho(\text{SD}, \text{DOY}, \text{SC}) = (\rho_{\max} - \rho_0)[1 - \exp(-k_1 \times \text{SD} - k_2 \times \text{DOY})] + \rho_0 \quad (3)$$

7 | where  $\rho_{\max}$  is the maximum density,  $\rho_0$  is the initial density,  $k_1$  and  $k_2$  are densification  
8 | parameters for SD and DOY, respectively.  $k_1$ ,  $k_2$ ,  $\rho_{\max}$ ,  $\rho_0$  vary with SC (Table 3). For operational  
9 | purposes in our work, DOY extend to 1 September each year (Matthew Sturm, personal  
10 | communication, 2018) running from -122 (1 September) to 181 (30 June). Sturm et al. (2010) didn't  
11 | compute snow density for the SC as ephemeral snow despite its presence in the Northern Hemisphere.  
12 | According to Zhong et al. (2014) study, the snow density of ephemeral is set to a fixed value, 0.25  
13 | g/cm<sup>3</sup>. Finally, daily snow density is simulated by the Eq. 3 in the Northern Hemisphere during the  
14 | 1992–2016 period.

## 15 | **4 Results and Discussion**

### 16 | **4.1 Snow depth**

#### 17 | **4.1.1 Validation of snow depth**

18 | Here to give insight into relative performance of SD products, we compared three sources of snow  
19 | cover product (NHSnow, GlobSnow, and ERA-Interim/Land) with ground SD observations (Fig. 5-7)  
20 | using three indices bias, mean absolute error (MAE) and root mean square error (RMSE).The common  
21 | period (1992 - 2010) daily SD of three products (Section 2.4) were collected as validation data. This  
22 | validation work primarily focus on snow cover stabilization stage (December to February). Since the  
23 | snow density change slowly over a smaller range in snow cover stabilization stage (Xiao et al., 2018),  
24 | using a constant value (0.24 g/cm<sup>3</sup>) for GlobSnow could introduce relative little error (Section 3.3).  
25 | Subject to the unavailability of SWE station observations, the evaluation of SWE can't be carried out.

26 | The relatively little bias (blue and green dots) between the estimated SD from three products

1 against measured SD is located in mid and low latitude regions ( $< 60^{\circ}\text{N}$ ) for these three snow depth  
2 datasets (NHSnow, GlobSnow, and ERA-Interim/Land; Fig. 5). However, a large bias was found in the  
3 polar region and along the coast, such as the north of Russia near the Arctic Ocean, Russian Far East,  
4 Korean peninsula, Northern Mediterranean and Northeast Canada. For NHSnow and GlobSnow, most  
5 bias is distributed near the  $\mu=0$  line with high frequency, although some bias is greater than 100 (or less  
6 than  $-100$ ) (Fig. 5b, d). Positive (negative) biases indicate mean grid cell values less (greater) than  
7 those of the respective stations SD measures. Fig. 5c showed the ERA-Interim/Land overestimate snow  
8 depth in Western Siberian Plains and Eastern European Plains (around  $60^{\circ}\text{N}$ ; orange dots). As  
9 reference, Average SD pattern of three products in February (1992-2010) were also provided in  
10 Appendix (Fig. A)

11 For analysis indexes, MAE and RMSE, the distribution of error points of NHSnow and GlobSnow  
12 are much the same as the distribution of its bias (Fig. 5-7). We used all evaluation records to calculate  
13 three precision indexes for three products. We found that the bias, MAE and RMSE is 0.59 cm, 15.12  
14 cm and 20.11 cm, respectively, for NHSnow gridded product, but more bias (1.19 cm), MAE (15.98 cm)  
15 and lower RMSE (15.48 cm) for GlobSnow (Table 4). This comparison (NHSnow vs. GlobSnow)  
16 showed relatively good agreement, although NHSnow over- or underestimated the SD with larger  
17 RMSE. Overall, the performance of GlobSnow was better than the NHSnow gridded product. However,  
18 part of the validation data were also applied for GlobSnow assimilation, it is highly possible that in this  
19 case GlobSnow validation may not completely independent. The different performance for these two  
20 products may be mainly because the evolution of snow grain size by HUT (The Helsinki University of  
21 Technology) model was used to generate SWE in GlobSnow. Che et al. (2016) reported that the grain  
22 size is more important than snow density and temperature. Further, ERA-Interim/Land had the worst  
23 performance of all three products with highest bias ( $-5.60$ ), MAE (18.72) and RMSE (37.77). The  
24 smallest bias is located near mid-latitude regions ( $< 50^{\circ}\text{N}$ ) and much of the bias lies at 0–100 cm for  
25 ERA-Interim/Land products (Fig. 5e, f). It must be noted that there are 89 bias records in two stations,  
26 which located in Novosibirsk Islands and Victoria Island, is much less than  $-300$  cm (approximately  
27  $-3000$  cm). Large MAE and RMSE can be found in high latitude and coastal region (Fig. 5e). Unlike  
28 NHSnow and GlobSnow, ERA-Interim/Land is more likely to overestimate SD and appears to be less  
29 consistent with in situ observation across the Northern Hemisphere (Fig. 5f). Through analyzing ground  
30 observation, we can see that deep snow is distributed in high latitude areas.

1 While the gridded products do a fairly good job of representing smaller accumulations of SD  
2 (shallow and mid-deep snow cover), they all struggle to capture very high accumulations (deep snow)  
3 with less bias, MAE and RMSE (Fig. 5-7, Fig. A). As a result, variation in snow cover could fail to be  
4 adequately captured in areas with frequent deep snow and, thus, we should be cautious when  
5 interpreting of this validation result.

6 Uncertainties in these three gridded snow products caused by ground temperature and topographic  
7 factor could result in some level discrepancies between the measured and the estimated SD (Vander  
8 Jagt et al., 2013; Snauffer et al., 2016). Forests exhibit strong influence on snow distributions by canopy  
9 interception and the evolution of snow properties. The dense portions of boreal forests are widely  
10 distributed in NA and northern EU (Friedl et al., 2010) Large bias, MAE and RMSE regions of three  
11 gridded products (Fig. 5-7) cover vast areas of tall vegetation (forests and shrub). Furthermore, the  
12 spatial inhomogeneity cause one grid cells (~25 km) that is almost not possible to completely cover by  
13 one vegetation type (low heterogeneity). Because the estimated SD of NHSnow depends on land cover  
14 types, this discrepancy induced by surface cover heterogeneity could partly account for why NHSnow  
15 has a smaller MAE and RMSE for low vegetation (bare-land and prairie) distributed at middle and low  
16 latitudes, than the higher vegetation (shrub and forest) areas at higher latitudes (Xiao et al., 2018).

17 As well, there are scale mismatches between in situ observation and the gridded products with  
18 regard to snowpack properties and their spatiotemporal representativeness (Frei et al., 2012). It is  
19 difficult to precisely validate coarse-resolution satellite observation using ground truth. Subsequently,  
20 over- or underestimates are inevitable when using a single in situ (SD or SWE) observation to test the  
21 veracity of the gridded products (Mudryk et al., 2015; Xiao et al., 2018). Snow surveys would benefit  
22 from multiple measurements at different points within one pixel (López-Moreno et al., 2011). In situ  
23 observations are highly representative when the SD varies smoothly in space, and poorly representative  
24 when the SD is spatially stepped (Che et al., 2016). However, there is almost always a lack of sufficient  
25 ground-measured data. To date, field site observations are still to be more authentic and reliable  
26 datasets than satellite observation.

27 As a whole, the accuracy of estimated SD in the Northern Hemisphere presented a spatial  
28 heterogeneity. Issues of scale and spatial heterogeneity of validation data notwithstanding, these  
29 comparisons conducted in our work can yield valuable insight into the performance of these products.

#### 1 4.1.2 Variation of snow depth

2 To better understand and interpret snow cover variation across the Northern Hemisphere, we  
3 conducted an analysis of SD variation using seasonal maximum SD from 1992–2016. According to the  
4 rules of variation level grading, which was divided into 5 grade (extremely significant decrease,  
5 significant decrease, non-significant change, extremely-significant increase, and extremely significant  
6 increase; Table 5), we can easily gained seasonal maximum SD variation level range 1992 to 2016.  
7 Figure 8 shows the variation pattern of seasonal maximum SD in three seasons (fall, winter and spring)  
8 with statistical significance level. In three seasons, variation trend of seasonal maximum SD exhibited a  
9 distinctly different pattern over the Northern Hemisphere since 1992. Seasonal maximum SD variation  
10 results in fall illustrated that a reduction trend account for most area of the EU with the rate ranging  
11 from 0 to 1 cm yr<sup>-1</sup>. The Figure 8a show the significant level pattern of corresponding maximum SD  
12 change trend. We can find that the area, which show extremely significant decrease in fall, are mainly  
13 located in the Russian Far East, the Qinghai-Tibet Plateau, the southern Siberian Plateau, and the  
14 northeastern region of Canada. On the contrary, Russia's Taimir Peninsula and the United States'  
15 Alaska region shows extremely significant increase trend (0 ~1 cm yr<sup>-1</sup>). In addition, the maximum SD  
16 in winter and spring also exhibited extremely significant decrease in the Qinghai-Tibet Plateau and the  
17 northeastern region of Canada as shown in Figure 8b and 8c. The area with extremely significant  
18 decrease trend extent add a Western Siberian plain region. Wang and Li (2012) used nearly 50a of daily  
19 station SD observation data to analyze the trend of maximum SD in China. The variation trend of  
20 seasonal maximum SD in the Qinghai-Tibet Plateau form previous study is consistent with the  
21 conclusion observed in this study (Wang and Li, 2012). There are more regions in seasonal maximum  
22 SD with extremely significant increase trend in winter and spring (green region). Furthermore, a  
23 strange phenomenon that the variation trend of seasonal maximum SD in the Russian Far East show  
24 extremely significant decrease, while it is in inverse in spring. This variation trend of maximum SD in  
25 spring analyzed using NHSnow products is consistent with the analysis results using GlobSnow  
26 products from recently published study (Wu et al., 2018). It need be pointed out that the significant  
27 increase (decrease) area is located around extremely significant increase (decrease) as shown in Figure  
28 8. No matter which season, although the variation trend of maximum seasonal SD didn't pass the  
29 significance level test, we can draw the conclusion that the wide range of area across the Northern

1 Hemisphere experienced pronounced change during the period 1992 to 2016.

2 Finally, we analyzed season variation analysis of SD across the Northern Hemisphere using  
3 seasonal average SD as analysis index (refer to Eq. A in Appendix). Seasonal average SD was defined  
4 as the cumulative SD divided by the days in one snow cover season. SD variation rate fluctuated in  
5 different regions and seasons. It was generally large in the region north of 55° N (Fig. 9, Fig. B and C  
6 in appendix). This fluctuation was large in winter with high of  $-0.11 \pm 0.40 \text{ cm yr}^{-1}$  than other seasons  
7 during 1992–2016 (Fig. 9d, Table 6.), which means that the maximum changes occurred in winter.  
8 Similar conclusion also can be easily found in the two periods 1992–2001 and 2002–2016 (Fig. B-d,  
9 C-d and Table 6). Although not all variation trends passed the significance test, most regions in the  
10 Northern Hemisphere show increasing trends during 1992-2001 (Fig. B; Table 6). The SD variation  
11 trend in the three seasons during 2002–2016 was reversed. The SD absolute variation rate during  
12 2002–2016 is apparently greater than its rate during 1992–2001 (Fig. C; Table 6). The last century were  
13 considered to be the warmest period.

14 The high fluctuation of SD variation rate especially occurred in the polar region (the arctic and the  
15 Tibetan plateau) for three seasons. In the context of global climate change, we found that winter SD  
16 variation was more sensitive to climate change (Brown et al., 2010). The strength of this relationship is  
17 spatially complex, varying by latitude, region, and climate condition.

## 18 **4.2 Snow mass**

19 GlobSnow dataset covers all land surface areas excluding mountainous regions, glaciers and  
20 Greenland as described in Section 2.4. From above analysis, we can find that ERA-Interim/Land have  
21 somewhat poor performance in SD estimation. Thus, further analysis of snow cover variation in the  
22 Northern Hemisphere used NHSnow products as analysis data. The forecast for snow mass have great  
23 potential consequences on agriculture practices in many regions. Snow mass in here is calculated by  
24 SWE multiplied by snow cover area (Qin et al., 2006). It should be noted that the snow classification  
25 tree (Grody and Basist, 1996), which have been applied in many studies (Che et al., 2008; Dai et al.,  
26 2017; Yu et al., 2012), was used to detect snow cover for NHSnow product. Liu et al. (2018) also  
27 reported that Grody's algorithm had higher positive predictive values and lower omission errors by  
28 testing snow cover mapping algorithms with the in situ SD over China. In this study, Annual) average  
29 (maximum, and minimum) in one snow cover year (excluded July and August) were calculated as

1 analysis indexes and also monthly average snow mass in 25 years.

2 The snow mass variation characteristic over the past 25 years were explored by interannual  
3 variation (Fig. 10) and intra-annual cycles (not show figure) of snow mass over the Northern  
4 Hemisphere . Figure 10 depicts the time series of interannual variation of annual maximum, average  
5 and minimum snow mass with respect to 1992–2016 period. The biggest value of annual maximum  
6 snow mass occurred in 1998–1999 up to 4875 km<sup>3</sup>, while the least was 3969 km<sup>3</sup> in 2007-2008. The  
7 annual maximum snow mass present particularly significant decreasing trends ( $P \leq 0.05$ ) during  
8 1992–2016, at the rate of approximately  $-19.88 \text{ km}^3 \text{ yr}^{-1}$  (Fig. 10A). Trend analysis reveals that  
9 annual maximum snow mass have a 8% reduction from 1992 to 2016. Note that it present a increase  
10 variation trend by about  $25.59 \text{ km}^3 \text{ yr}^{-1}$  ( $P > 0.05$ ) rate for 1992-2001. In contrast, the annual  
11 maximum snow mass exhibits a significantly decrease trends (with  $-34.80 \text{ km}^3 \text{ yr}^{-1}$ ,  $P \leq 0.05$ ) since  
12 2002, which would lead to a extraordinary decrease during 1992–2016. According to the static, the  
13 annual maximum snow mass usually appear in February (about 60%) and March (about 40%), and in  
14 recent several years this occurred in March become a normal state. [This finding need to be further](#)  
15 [analyzed in the future work by correlation with climatic factors, such as precipitation effects](#) (Kumar  
16 et al., 2012). We can find that the biggest and the least value of annual average snow mass  
17 respectively appear in 1998-1999 ( $\sim 2370 \text{ km}^3$ ) and 2015-2016 ( $\sim 1850 \text{ km}^3$ ) in Fig 10B. Likewise, in  
18 Fig 10B and 10C the annual average (minimum) snow mass exhibit a significant decrease trend in  
19 1992-2016 period by rate  $-19.72 \text{ km}^3 \text{ yr}^{-1}$ ,  $P > 0.05$  ( $-2.00 \text{ km}^3 \text{ yr}^{-1}$ ,  $P \leq 0.05$ ) and 2002-2016 period at  
20 a rate of  $-30.70 \text{ km}^3 \text{ yr}^{-1}$ ,  $P > 0.05$  ( $-2.2 \text{ km}^3 \text{ yr}^{-1}$ ,  $P \leq 0.05$ ). For 1992-2016 period, the variation  
21 tendency of annual average (minimum) snow mass do not pass the significance level test. Moreover,  
22 the reduction for the annual average and annual minimum snow mass is 13% and 67%, respectively.  
23 Other factors, for instance, oceanic and atmospheric heat transport, sea ice season wind, and solar  
24 insolation anomalies, may have contributed to the fluctuation of snow mass (Liu and Key, 2014).  
25 Variation of snow mass across the Northern Hemisphere could well capture the variation characteristic  
26 of the Arctic sea ice extent (Tilling et al., 2015).

27 When analyzing long-term variation of monthly average snow mass ([refer to Eq. B in Appendix](#)),  
28 ten months (September to June) exhibit significant decreasing apart from March and April (Table 7).  
29 The maximum decrease rate was approximately  $-36.50 \text{ km}^3 \text{ yr}^{-1}$  ( $P \leq 0.05$ ) in November while the  
30 minimum decrease occurred in April at  $-4.29 \text{ km}^3 \text{ yr}^{-1}$  ( $P > 0.05$ ). [However, there are no significant](#)

1 trends in March and April with large interannual variations (Table 7).~~An increasing trend appears in~~  
2 ~~March with a rate of approximately  $1.90 \text{ km}^3 \text{ yr}^{-1}$  ( $P > 0.05$ ), however, relatively large decrement in~~  
3 ~~fall and winter are unable to partially be offset by the increment of March.~~ Compared with the fall  
4 (September to November) and spring (March to June), the interannual variability of monthly average  
5 snow mass significantly decreased in winter (December to February), with average rate of less than  
6  $-32 \text{ km}^3 \text{ yr}^{-1}$ . The reduction of monthly average snow mass in ten month were generated using the  
7 average pattern of each month over 1992-2016 as a reference. We found that the reduction of monthly  
8 average snow mass fluctuated ranging from -65% to -4% for each month (September to June) over  
9 1992-2016 (Table 7). The largest and smallest reduction were about 64.67% and 4.30%, which  
10 occurred in June and March, respectively. Variation analysis of monthly average snow mass could  
11 offer a powerful evidence for annual average snow mass exhibit a significantly decreasing tendency  
12 (Table 7, Fig. 10B).

13 Over large areas, it is extremely convenient to use remote sensing to infer SWE. Albeit there are  
14 numerous ways to estimate SWE, it is very challenging to determine precise distributions of SWE at  
15 regional and global scales (Chang et al., 1987;Kongoli, 2004;Tedesco and Narvekar, 2010;Bair et al.,  
16 2018). Snow density, which can be used to convert SWE from SD, is potential and key factor in  
17 accurate estimation of SWE (Sturm et al., 2010;Tedesco and Narvekar, 2010). In fact, snow density  
18 typically varies from  $0.05 \text{ g/cm}^3$  for new snow at low air temperatures to over  $0.55 \text{ g/cm}^3$  for a ripened  
19 snowpack (Anderton et al., 2004;Cordisco et al., 2006). Noteworthily, this study using dynamic snow  
20 density to convert SD to SWE is based on the assumption that snowpack occurs as a single layer  
21 (Sturm et al., 2010), to capture dynamic characteristics of snow property. The evolution of the  
22 ephemeral snow class did not be provided by Sturm et al. (2010). The mean value ( $0.25 \text{ g/cm}^3$ ) of snow  
23 density of ephemeral snow (Zhong et al., 2014), which mean that without any evolution throughout the  
24 snow cover year. Meanwhile, this value for ephemeral snow was set as  $0.2275 \text{ g/cm}^3$  in Tedesco and  
25 Jeyaratnam (2016) study. Snow density also exhibits great heterogeneity in vertical direction, so that a  
26 single layer of snow concept cannot fully capture the snowpack property. The density of the top  
27 snowpack (fresh snow;  $\sim 0.10 \text{ g/cm}^3$ ) increases gradually from the top toward the bottom (Dai et al.,  
28 2012). The bottom layer of snowpack is old undergoing compaction and grain size growth with a  
29 relatively high density ( $0.3\sim 0.6 \text{ g/cm}^3$ ). Although our snow density description strategy does not  
30 completely describe the actual evolution in snow density, there is no better alternative.

### 1 4.3 Snow cover days

2 Snow cover days (SCD) is defined as the number of days in one snow cover year in which SD is  
3 over 0 cm (Zhong, 2014). Snow cover year was defined as the period between July of a given year and  
4 June of the following year (Xiao et al., 2018). A least-squares regression was used to analyze the  
5 variation of SCD for each pixel from 24 snow cover years, with per-pixel evaluation of significance  
6 (F-test).

7 We exploring the variation in SCD during 1992-2016. Most areas across the Northern Hemisphere  
8 present a prominently decreasing trend at a rate ranging from 0 to 5 day yr.<sup>-1</sup> (Fig. 11a). Decreasing  
9 regions are mainly distributed in EU. For example, north of Russia and large parts of central Asia. The  
10 area that shows decreasing trends of SCD in EU is much larger than that in NA (Fig. 11a) (Derksen and  
11 Brown, 2012). Areas that the decrease at a rate greater than 5 day yr.<sup>-1</sup> are almost all located in China,  
12 such as North of Qilian Mountain, central Tibetan Plateau, and Tianshan Mountain. Areas that exhibits  
13 increasing trends, can be found in central of NA, Western Europe, Northwestern Mongolia, and some  
14 parts of China. Throughout the Northern Hemisphere (Fig. 11b), the decreasing trend covered most  
15 parts of the regions (25 ~ 85 °N) with a mean decreasing rate of approximately 1.0 day yr.<sup>-1</sup>. Latitudes  
16 around 50 °N is an exception where variation is close to 0 day yr.<sup>-1</sup>. The most notable variation trend  
17 (decreasing or increasing) occurred over polar region (Fig. 11b). This may be because there are few  
18 pixels in the polar mainland.

19 SCD variation rate also were divided into 5 grade (Table 5). Unlike SCD variation rate patterns,  
20 the variation level pattern shows that the non-significant changes area dominates SCD variation trends  
21 across the Northern Hemisphere (Fig. 11c). Extremely significant and significant decrease appear in  
22 northwest of Hudson Bay in Canada, Kamchatka peninsula, Eastern European plains, the north of  
23 Russia, Iranian plateau, and several regions in China (the Tibet Plateau, Tianshan Mountain and  
24 Northeast China Plain). In addition, extremely significant and significant increase only occur in a  
25 limited area of NA, eastern Tibet Plateau regions, and China's central and northern regions.

26 Interestingly, the opposite variation trends in SCD and SD appear in several regions. Maximum  
27 SD in spring (Fig. 8c) and annual average SD (figure not shown) show extremely significant increasing  
28 trends, whereas SCD exhibit extremely significant decreases in corresponding regions (Fig. 11c), such  
29 as Central Siberian Plateau, Greater Khingan Mountains in China, and the eastern Scandinavian

1 Peninsula. This different variation trend of SD and SCD was also reported by Zhong et al. (2018) using  
2 ground-based data. The primary reason may be the increase of frequency of extreme snowfall in which  
3 SD could demonstrate on increasing trend. Additionally, a recent study found that the greater SWE, the  
4 faster melting rate leading to a shortened SCD in Northern Hemisphere (Wu et al., 2018).

5 Despite the similarities between the station- and satellite-derived time series, it can be  
6 demonstrated that Northern Hemisphere meteorological station data do not provide perfect large-scale  
7 variation characteristics of ground snow cover (Zhong et al., 2018). Our analyses provide further  
8 evidence supporting observations of significant decreasing trends in SCD occurring in the Northern  
9 Hemisphere. Compared to SCD derived from optic sensors snow cover product, however, the specific  
10 quantity of SCD and SCD variation rate derived from NHSnow SD data was overestimated (Wang et  
11 al., 2018;Hori et al., 2017). The SCD variation trends derived from NHSnow product almost is same as  
12 derived from optical snow cover product in variation pattern (Hori et al., 2017).

13 Since the optical (MODIS or AVHRR) and microwave sensors (SSM/I or AMSR-E) respond in  
14 different parts of the electromagnetic spectrum, the estimated snow cover will to be somewhat vary.  
15 The shallow snow could not induce volume scattering at 37 GHz, and thus passive microwave  
16 observations often give better snow cover result at thick snow (>5 cm) (Foster et al., 2009;Wang et al.,  
17 2008). The threshold for SCD definition in here is 0 cm, whereas it is 1 cm or larger in other studies  
18 (Ke et al., 2016;Dyer and Mote, 2006). As well, another explanation for these discrepancy could be  
19 snow cover identification algorithm (Liu et al., 2018;Hall et al., 2002).

20 The microwave radiation characteristics of snow cover is similar to that of precipitation, cold  
21 desert and, frozen ground (Grody and Basist, 1996). Commission and omission errors in NHSnow  
22 product may result from coarse spatial resolution, snow characteristics and topography according to  
23 Dai et al. (2017), precipitation (Liu et al., 2018;Grody and Basist, 1996) especially over frozen ground  
24 (Tsutsui and Koike, 2012). Algorithm several rules were used to distinguish snow from precipitation,  
25 cold desert, and frozen ground (Xiao et al., 2018), it is impossible to entirely remove interference  
26 factors in each image. Additionally, the precondition of NHSnow is dry snow, which mean almost no  
27 wet snow was considered into SCD variation analysis (Singh and Gan, 2000). The poorer performance  
28 of the microwave derived products was anticipated because of documented difficulties monitoring  
29 snow cover over forested and mountainous terrain (Vander Jagt et al., 2013;Smith and Bookhagen,  
30 2016).

## 1 **5 Conclusions**

2 This project applied the SVR SD retrieval algorithm proposed by Xiao et al (2018), which using  
3 PM remote sensing and other auxiliary data, to develop a long term (from January 1992 to December  
4 2016) Northern Hemisphere daily SD and SWE products (NHSnow) with 25-km spatial resolution. We  
5 then analyzed the spatial and temporal change in snow cover (SD, snow mass and, SCD) across the  
6 Northern Hemisphere, and quantified the magnitude of variation of snow cover using SD and SWE  
7 extracted from NHSnow product.

8 In this study, we validated and compared among daily gridded products (NHSnow, GlobSnow and  
9 ERA-Interim/Land) against ground snow-depth observations. The results show relatively high  
10 estimation accuracy of SD from NHSnow, providing the relatively little bias, RMSE, and MAE  
11 between the newly SD products and in situ observation. Analysis of SD variation revealed that the  
12 variation rate ranging from 0 to 1 cm yr.<sup>-1</sup> (negative and positive) dominates the change in the Northern  
13 Hemisphere, and the maximum changes appear in winter. Additionally, the results revealed the overall  
14 SD trends in three seasons show increasing trend during 1992–2001, however it has a decreasing trend  
15 during 2002–2016. Similar conclusions also appear in snow mass change analysis. The annual  
16 maximum, average and minimum snow mass exhibit significantly decrease trends and respectively  
17 show a 8%, 13% and 67% reduction. The monthly average snow mass has shown a decreasing trend  
18 almost in every month and the reduction range from 64.67% (June) to 4.3% (March). The annual  
19 average snow mass report well-documented significant decreasing trends ( $\sim 20 \text{ km}^3 \text{ yr}^{-1}$ ,  $P < 0.05$ )  
20 during the study period. Regression analysis multi-year Northern Hemisphere SCD exhibits a  
21 prominent decreasing trend at a rate ranging from 0 to 5 day yr.<sup>-1</sup>. The area of decreasing trends of SCD  
22 in EU is much larger than in NA. Unlike the SCD variation rate, its variation level shows that  
23 non-significant changes areas dominate the variation pattern across the Northern Hemisphere. An  
24 abnormal and interesting phenomenon is that opposite SCD and SD variation trends appear in several  
25 regions.

26 While this study shed light on the spatiotemporal variability trends of snow cover across the  
27 Northern Hemisphere using 25-year NHSnow product, we cannot claim NHSnow dataset could  
28 completely capture the climate change signal in each region and season. Because of the deficiencies  
29 and limitations (e.g. overestimation, underestimation), further efforts should be made to improve the

1 estimation accuracy and robustness of the SD inversion algorithm. Additionally, when more reliable  
2 and numerous data become available, we will do more comprehensive validation over higher latitudes  
3 and mountainous regions (Dai et al., 2017). Meanwhile, the validation analysis also should be carried  
4 out in complex terrain and different land cover types (Tennant et al., 2017; Snauffer et al., 2016). It is  
5 recommended that future work focus on the climatic effects and climatological causes in snow cover  
6 changes to comprehensively understand the associated snow cover change mechanisms against a  
7 climate change background (Huang et al., 2017; Flanner et al., 2011; Cohen et al., 2012).

## 8 Acknowledgments

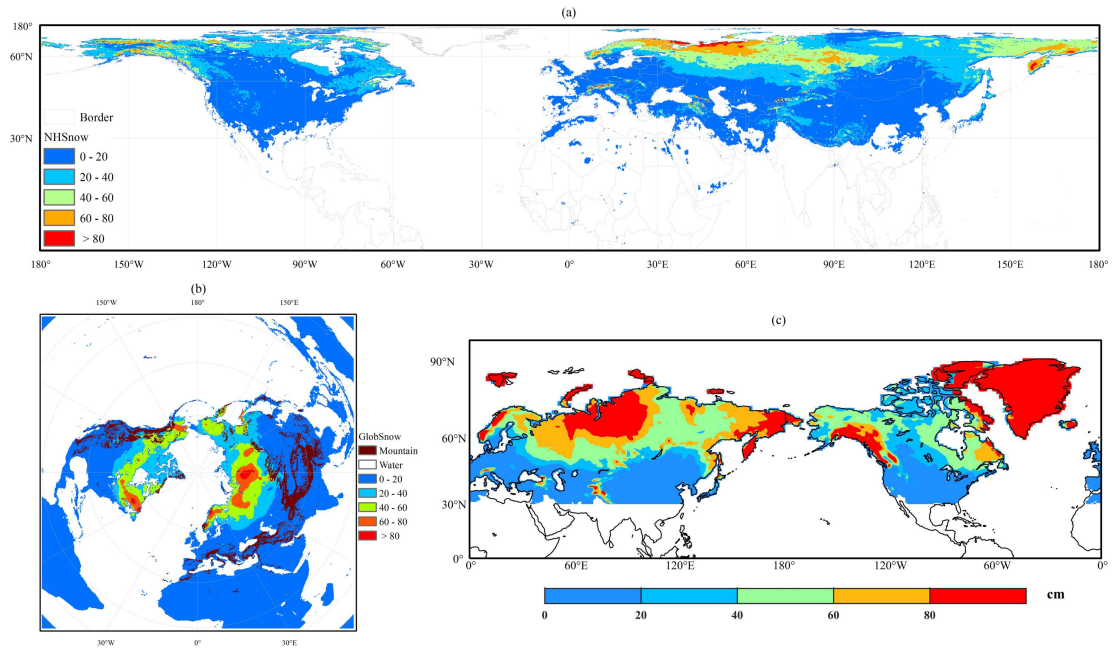
9 This study was funded by the National Natural Science Foundation of China (grant nos. 91325202;  
10 41871050; 41801028), National Key Scientific Research Program of China (grant no. 2013CBA01802),  
11 and the Strategic Priority Research Program of Chinese Academy of Sciences (grant nos.  
12 XDA20100103; XDA20100313).

## 13 Appendix

$$SD_{average} = \frac{\sum_{i=1}^n SD_i}{n} \quad (A)$$

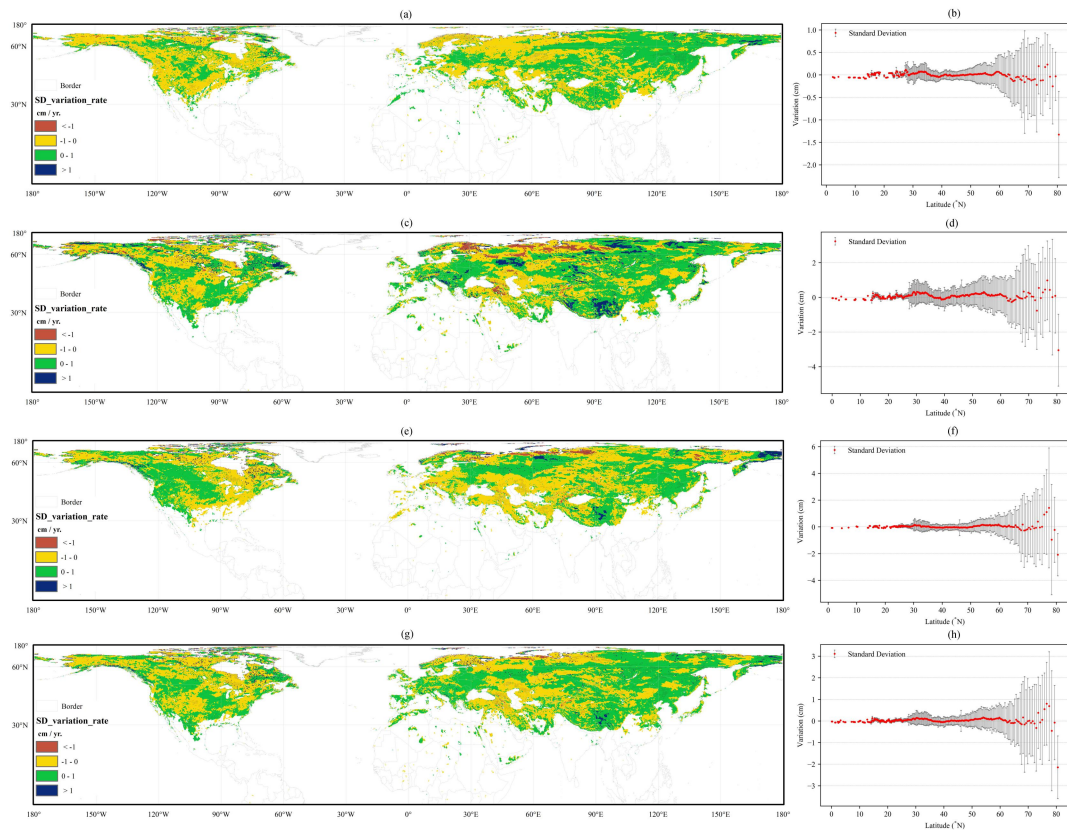
$$SM_{average} = \frac{\sum_{i=1}^n SM_i}{n} \quad (B)$$

14 Where  $n$  is the number of days in one specific period of time (one month, or snow cover year/season),  $i$   
15 is  $i$ th day in one specific period of time (one month, or snow cover year/season). SD is snow depth. SM  
16 is snow mass.  
17



1  
2  
3  
4

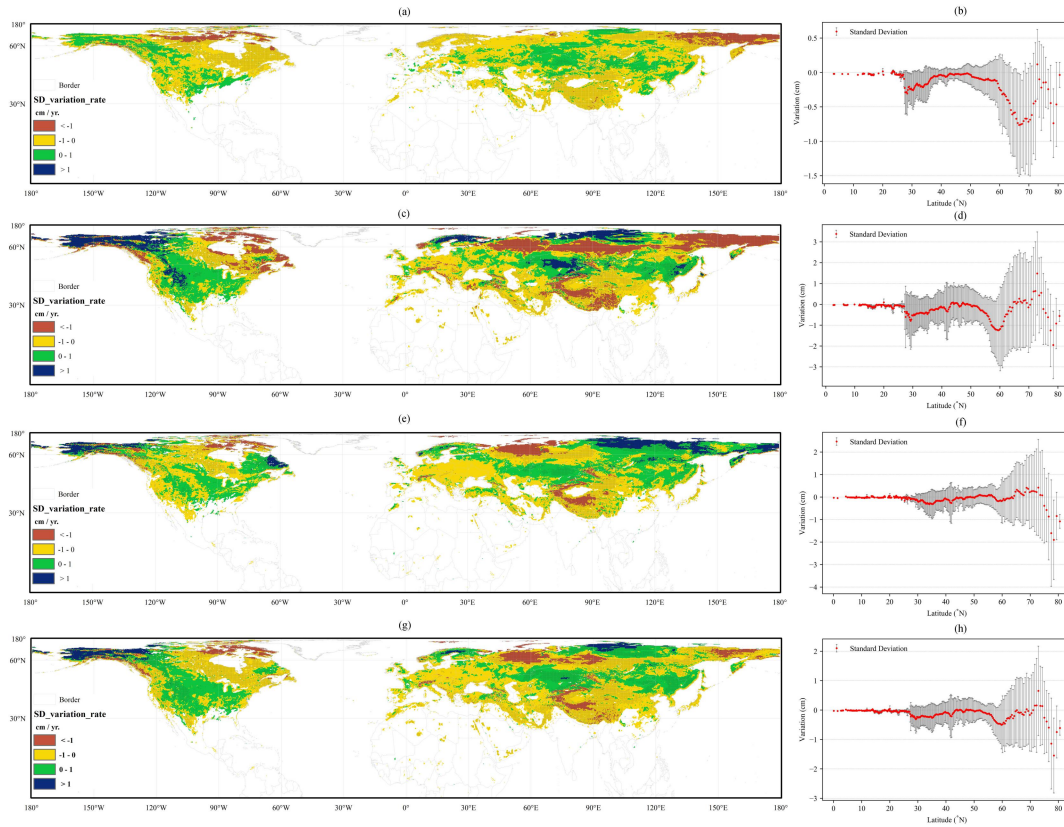
Figure A. Monthly average snow depth climatology of three products in February during 1992-2010: a) NHSnow; b) GlobSnow, c) ERA-Interim/Land



5  
6

Figure B. The variation rate pattern of annual average (season) SD over the Northern Hemisphere for

1 three snow cover season, fall (a, b; September to November), winter (c, d; December to February),  
 2 spring (e, f; March to June) from 1992-2001. Black dots in (a, c, e, g) indicate that the changes are  
 3 significant at 95% confidence level (CL). The zonal distribution in (b, d, f, h) are mapped at 0.25  
 4 degree resolution in latitude. The error bars in (b, d, f, h) is one times of standard deviation.



5  
 6 Figure C. The variation rate pattern of annual (season) average SD over the Northern Hemisphere for  
 7 three snow cover season, fall (a, b; September to November), winter (c, d; December to February),  
 8 spring (e, f; March to June) from 2002-2016. Black dots in (a, c, e, g) indicate that the changes are  
 9 significant at 95% confidence level (CL). The zonal distribution in (b, d, f, h) are mapped at 0.25  
 10 degree resolution in latitude. The error bars in (b, d, f, h) is one times of standard deviation.

11

1

Table A. AVHRR Global Land Cover classification and reclassification schemes

Value	Classification Label	Reclassification Label
0	Water	Water
1	Evergreen needle leaf forest	Forest
2	Evergreen broad leaf forest	
3	Deciduous needle leaf forest	
4	Deciduous broad leaf forest	
5	Mixed forest	
6	Woodland	
7	Wooded grassland	Prairie (Grassland)
10	Grassland	
8	Closed shrub land	Shrub
9	Open shrub land	
11	Cropland	Bare-land
12	Bare ground	
13	Urban and built	

2

1 References

- 2 Amante, C., Eakins, B.W.: ETOPO1 1 arc-minute global relief model: procedures, data sources and  
3 analysis, US Department of Commerce, National Oceanic and Atmospheric Administration, National  
4 Environmental Satellite, Data, and Information Service, National Geophysical Data Center, Marine  
5 Geology and Geophysics Division Colorado, 2009.
- 6 Anderton, S. P., White, S. M., and Alvera, B.: Evaluation of spatial variability in snow water equivalent  
7 for a high mountain catchment, *Hydrological Processes*, 18, 435-453, 10.1002/hyp.1319, 2004.
- 8 Armstrong, R., and Brodzik, M.: An earth-gridded SSM/I data set for cryospheric studies and global  
9 change monitoring, *Advances in Space Research*, 16, 155-163, 1995.
- 10 Armstrong, R. L., Knowles, K.W., Brodzik, M.J., Hardman, M.A.: DMSP SSM/I pathfinder daily  
11 EASE-grid brightness temperatures, Boulder, Colorado USA: National snow and ice data center,  
12 Digital media, 2008.
- 13 Bair, E. H., Andre Calfa, A., Rittger, K., and Dozier, J.: Using machine learning for real-time estimates  
14 of snow water equivalent in the watersheds of Afghanistan, *The Cryosphere*, 12, 1579-1594,  
15 10.5194/tc-12-1579-2018, 2018.
- 16 Balsamo, G., Albergel, C., Beljaars, A., Boussetta, S., Brun, E., Cloke, H., Dee, D., Dutra, E.,  
17 Munoz-Sabater, J., and Papenberger, F.: ERA-Interim/Land: A global land surface reanalysis dataset,  
18 European Geosciences Union General Assembly, 2015, 389-407,
- 19 Barnett, T. P., Adam, J. C., and Lettenmaier, D. P.: Potential impacts of a warming climate on water  
20 availability in snow-dominated regions, *Nature*, 438, 303-309, 10.1038/nature04141, 2005.
- 21 Barrett, B. S., Henderson, G. R., and Werling, J. S.: The Influence of the MJO on the Intraseasonal  
22 Variability of Northern Hemisphere Spring Snow Depth, *Journal of Climate*, 28, 7250-7262,  
23 10.1175/jcli-d-15-0092.1, 2015.
- 24 Bilello, M. A.: Regional and seasonal variations in snow-cover density in the U.S.S.R, 1984.
- 25 Brodzik, M. J., and Knowles, K.: EASE-Grid: A Versatile Set of Equal-Area Projections and Grids,  
26 2002.
- 27 Brown, R., Derksen, C., and Wang, L.: A multi-data set analysis of variability and change in Arctic  
28 spring snow cover extent, 1967–2008, *Journal of Geophysical Research*, 115, 10.1029/2010jd013975,  
29 2010.
- 30 Brown, R., and Robinson, D.: Northern Hemisphere spring snow cover variability and change over  
31 1922–2010 including an assessment of uncertainty, *The Cryosphere*, 5, 219-229, 2011.
- 32 Brown, R. D., and Frei, A.: Comment on “Evaluation of surface albedo and snow cover in AR4 coupled  
33 models” by A. Roesch, *Journal of Geophysical Research*, 112, 10.1029/2006jd008339, 2007.
- 34 Chang, A., Foster, J., and Hall, D.: Nimbus-7 SMMR derived global snow cover parameters, *Ann.*  
35 *Glaciol*, 9, 39-44, 1987.
- 36 Che, T., Xin, L., Jin, R., Armstrong, R., and Zhang, T.: Snow depth derived from passive microwave  
37 remote-sensing data in China, *Annals of Glaciology*, 49, 145-154, 2008.
- 38 Che, T., Dai, L., Zheng, X., Li, X., and Zhao, K.: Estimation of snow depth from passive microwave  
39 brightness temperature data in forest regions of northeast China, *Remote Sensing of Environment*, 183,  
40 334-349, 2016.
- 41 Cohen, J. L., Furtado, J. C., Barlow, M. A., Alexeev, V. A., and Cherry, J. E.: Arctic warming,  
42 increasing snow cover and widespread boreal winter cooling, *Environmental Research Letters*, 7,  
43 10.1088/1748-9326/7/1/014007, 2012.
- 44 Cordisco, E., Prigent, C., and Aires, F.: Snow characterization at a global scale with passive microwave

1 satellite observations, *Journal of Geophysical Research*, 111, 10.1029/2005jd006773, 2006.

2 Dai, L., Che, T., Wang, J., and Zhang, P.: Snow depth and snow water equivalent estimation from  
3 AMSR-E data based on a priori snow characteristics in Xinjiang, China, *Remote Sensing of*  
4 *Environment*, 127, 14-29, 2012.

5 Dai, L., Che, T., and Ding, Y.: Inter-calibrating SMMR, SSM/I and SSMI/S data to improve the  
6 consistency of snow-depth products in China, *Remote Sensing*, 7, 7212-7230, 2015.

7 Dai, L., Che, T., Ding, Y., and Hao, X.: Evaluation of snow cover and snow depth on the  
8 Qinghai-Tibetan Plateau derived from passive microwave remote sensing, *The Cryosphere*, 11,  
9 1933-1948, 10.5194/tc-11-1933-2017, 2017.

10 Derksen, C., Walker, A., and Goodison, B.: Evaluation of passive microwave snow water equivalent  
11 retrievals across the boreal forest/tundra transition of western Canada, *Remote Sensing of Environment*,  
12 96, 315-327, 2005.

13 Derksen, C., and Brown, R.: Spring snow cover extent reductions in the 2008-2012 period exceeding  
14 climate model projections, *Geophysical Research Letters*, 39, n/a-n/a, 10.1029/2012gl053387, 2012.

15 Diffenbaugh, N. S., Scherer, M., and Ashfaq, M.: Response of snow-dependent hydrologic extremes to  
16 continued global warming, *Nat Clim Chang*, 3, 379-384, 10.1038/nclimate1732, 2013.

17 Dutra, E., Balsamo, G., Viterbo, P., Miranda, P. M. A., Beljaars, A., Schär, C., and Elder, K.: An  
18 improved snow scheme for the ECMWF land surface model: description and offline validation, *Journal*  
19 *of Hydrometeorology*, 11, 899-916, 2010.

20 Dyer, J. L., and Mote, T. L.: Spatial variability and trends in observed snow depth over North America,  
21 *Geophysical Research Letters*, 33, 10.1029/2006gl027258, 2006.

22 Flanner, M. G., Shell, K. M., Barlage, M., Perovich, D. K., and Tschudi, M. A.: Radiative forcing and  
23 albedo feedback from the Northern Hemisphere cryosphere between 1979 and 2008, *Nature*  
24 *Geoscience*, 4, 151-155, 10.1038/ngeo1062, 2011.

25 Forman, B. A., Reichle, R. H., and Derksen, C.: Estimating Passive Microwave Brightness Temperature  
26 Over Snow-Covered Land in North America Using a Land Surface Model and an Artificial Neural  
27 Network, *IEEE Transactions on Geoscience & Remote Sensing*, 52, 235-248, 2013.

28 Forman, B. A., and Reichle, R. H.: Using a support vector machine and a land surface model to  
29 estimate large-scale passive microwave brightness temperatures over snow-covered land in North  
30 America, *IEEE Journal of Selected Topics in Applied Earth Observations and Remote Sensing*, 8,  
31 4431-4441, 2015.

32 Foster, J., Chang, A., and Hall, D.: Comparison of snow mass estimates from a prototype passive  
33 microwave snow algorithm, a revised algorithm and a snow depth climatology, *Remote sensing of*  
34 *environment*, 62, 132-142, 1997.

35 Foster, J. L., Hall, D. K., Kelly, R. E. J., and Chiu, L.: Seasonal snow extent and snow mass in South  
36 America using SMMR and SSM/I passive microwave data (1979–2006), *Remote Sensing of*  
37 *Environment*, 113, 291-305, 10.1016/j.rse.2008.09.010, 2009.

38 Foster, J. L., Hall, D. K., Eylander, J. B., Riggs, G. A., Nghiem, S. V., Tedesco, M., Kim, E., Montesano,  
39 P. M., Kelly, R. E. J., Casey, K. A., and Choudhury, B.: A blended global snow product using visible,  
40 passive microwave and scatterometer satellite data, *International Journal of Remote Sensing*, 32,  
41 1371-1395, 10.1080/01431160903548013, 2011.

42 Frei, A., Tedesco, M., Lee, S., Foster, J., Hall, D. K., Kelly, R., and Robinson, D. A.: A review of global  
43 satellite-derived snow products, *Advances in Space Research*, 50, 1007-1029,  
44 10.1016/j.asr.2011.12.021, 2012.

1 Friedl, M. A., Sulla-Menashe, D., Tan, B., Schneider, A., Ramankutty, N., Sibley, A., and Huang, X.:  
2 MODIS Collection 5 global land cover: Algorithm refinements and characterization of new datasets,  
3 *Remote Sensing of Environment*, 114, 168-182, 2010.

4 Friedl, M. A., and Sulla-Menashe, D.: Note to users of MODIS Land Cover (MCD12Q1) Products,  
5 Report. Accessed March, 2, 2014, 2011.

6 Gan, T. Y., Barry, R. G., Gizaw, M., Gobena, A., and Balaji, R.: Changes in North American snowpacks  
7 for 1979–2007 detected from the snow water equivalent data of SMMR and SSM/I passive microwave  
8 and related climatic factors, *Journal of Geophysical Research: Atmospheres*, 118, 7682-7697, 2013.

9 Gharaei-Manesh, S., Fathzadeh, A., and Taghizadeh-Mehrjardi, R.: Comparison of artificial neural  
10 network and decision tree models in estimating spatial distribution of snow depth in a semi-arid region  
11 of Iran, *Cold Regions Science and Technology*, 122, 26-35, 2016.

12 Goïta, K., Walker, A. E., and Goodison, B. E.: Algorithm development for the estimation of snow water  
13 equivalent in the boreal forest using passive microwave data, *International Journal of Remote Sensing*,  
14 24, 1097-1102, 2003.

15 Grippa, M., Mognard, N., Le Toan, T., and Josberger, E.: Siberia snow depth climatology derived from  
16 SSM/I data using a combined dynamic and static algorithm, *Remote sensing of environment*, 93, 30-41,  
17 2004.

18 Grody, N. C., and Basist, A. N.: Global identification of snowcover using SSM/I measurements, *IEEE*  
19 *Transactions on geoscience and remote sensing*, 34, 237-249, 1996.

20 Hall, D. K., Kelly, R. E. J., Riggs, G. A., Chang, A. T. C., and Foster, J. L.: Assessment of the relative  
21 accuracy of hemispheric-scale snow-cover maps, *Annals of Glaciology*, 34, 24-30, 2002.

22 Hancock, S., Baxter, R., Evans, J., and Huntley, B.: Evaluating global snow water equivalent products  
23 for testing land surface models, *Remote sensing of environment*, 128, 107-117,  
24 10.1016/j.rse.2012.10.004, 2013.

25 Hansen, M. C., Defries, R. S., Townshend, J. R. G., and Sohlberg, R.: Global land cover classification  
26 at 1 km spatial resolution using a classification tree approach, *International Journal of Remote Sensing*,  
27 21, 1331-1364, 2000.

28 Hori, M., Sugiura, K., Kobayashi, K., Aoki, T., Tanikawa, T., Kuchiki, K., Niwano, M., and Enomoto,  
29 H.: A 38-year (1978–2015) Northern Hemisphere daily snow cover extent product derived using  
30 consistent objective criteria from satellite-borne optical sensors, *Remote Sensing of Environment*, 191,  
31 402-418, 10.1016/j.rse.2017.01.023, 2017.

32 Huang, X., Deng, J., Ma, X., Wang, Y., Feng, Q., Hao, X., and Liang, T.: Spatiotemporal dynamics of  
33 snow cover based on multi-source remote sensing data in China, *The Cryosphere*, 10, 2453-2463,  
34 10.5194/tc-10-2453-2016, 2016.

35 Huang, X., Deng, J., Wang, W., Feng, Q., and Liang, T.: Impact of climate and elevation on snow cover  
36 using integrated remote sensing snow products in Tibetan Plateau, *Remote Sensing of Environment*,  
37 190, 274-288, 10.1016/j.rse.2016.12.028, 2017.

38 Immerzeel, W. W., Van Beek, L. P., and Bierkens, M. F.: Climate Change Will Affect the Asian Water  
39 Towers, *Science*, 328, 1382-1385, 2010.

40 Ke, C.-Q., Li, X.-C., Xie, H., Ma, D.-H., Liu, X., and Kou, C.: Variability in snow cover phenology in  
41 China from 1952 to 2010, *Hydrology and Earth System Sciences*, 20, 755-770,  
42 10.5194/hess-20-755-2016, 2016.

43 Kongoli, C.: Interpretation of AMSU microwave measurements for the retrievals of snow water  
44 equivalent and snow depth, *Journal of Geophysical Research*, 109, 10.1029/2004jd004836, 2004.

1 Kumar, M., Wang, R., and Link, T. E.: Effects of more extreme precipitation regimes on maximum  
2 seasonal snow water equivalent, *Geophysical Research Letters*, 39, 10.1029/2012gl052972, 2012.

3 Li, W., Guo, W., Qiu, B., Xue, Y., Hsu, P. C., and Wei, J.: Influence of Tibetan Plateau snow cover on  
4 East Asian atmospheric circulation at medium-range time scales, *Nat Commun*, 9, 4243,  
5 10.1038/s41467-018-06762-5, 2018.

6 Liang, J., Liu, X., Huang, K., Li, X., Shi, X., Chen, Y., and Li, J.: Improved snow depth retrieval by  
7 integrating microwave brightness temperature and visible/infrared reflectance, *Remote Sensing of*  
8 *Environment*, 156, 500-509, 2015.

9 Liu, X., Jiang, L., Wu, S., Hao, S., Wang, G., and Yang, J.: Assessment of Methods for Passive  
10 Microwave Snow Cover Mapping Using FY-3C/MWRI Data in China, *Remote Sensing*, 10,  
11 10.3390/rs10040524, 2018.

12 Liu, Y., and Key, J. R.: Less winter cloud aids summer 2013 Arctic sea ice return from 2012 minimum,  
13 *Environmental Research Letters*, 9, 10.1088/1748-9326/9/4/044002, 2014.

14 López-Moreno, J. I., Fassnacht, S. R., Beguería, S., and Latron, J. B. P.: Variability of snow depth at the  
15 plot scale: implications for mean depth estimation and sampling strategies, *The Cryosphere*, 5, 617-629,  
16 10.5194/tc-5-617-2011, 2011.

17 Mudryk, L. R., Derksen, C., Kushner, P. J., and Brown, R.: Characterization of Northern Hemisphere  
18 Snow Water Equivalent Datasets, 1981–2010, *Journal of Climate*, 28, 8037-8051,  
19 10.1175/jcli-d-15-0229.1, 2015.

20 Pulliainen, J.: Mapping of snow water equivalent and snow depth in boreal and sub-arctic zones by  
21 assimilating space-borne microwave radiometer data and ground-based observations, *Remote Sensing*  
22 *of Environment*, 101, 257-269, 2006.

23 Qin, D., Liu, S., and Li, P.: Snow cover distribution, variability, and response to climate change in  
24 western China, *J. Climate*, 19, 1820-1833, 2006.

25 Robinson, D. A., and Frei, A.: Seasonal variability of Northern Hemisphere snow extent using visible  
26 satellite data, *The Professional Geographer*, 52, 307-315, 2000.

27 Rupp, D. E., Mote, P. W., Bindoff, N. L., Stott, P. A., and Robinson, D. A.: Detection and Attribution of  
28 Observed Changes in Northern Hemisphere Spring Snow Cover, *Journal of Climate*, 26, 6904-6914,  
29 10.1175/jcli-d-12-00563.1, 2013.

30 Singh, P. R., and Gan, T. Y.: Retrieval of snow water equivalent using passive microwave brightness  
31 temperature data, *Remote Sensing of Environment*, 74, 275-286, 2000.

32 Smith, T., and Bookhagen, B.: Assessing uncertainty and sensor biases in passive microwave data  
33 across High Mountain Asia, *Remote Sensing of Environment*, 181, 174-185, 2016.

34 Snauffer, A. M., Hsieh, W. W., and Cannon, A. J.: Comparison of gridded snow water equivalent  
35 products with in situ measurements in British Columbia, Canada, *Journal of Hydrology*, 541, 714-726,  
36 10.1016/j.jhydrol.2016.07.027, 2016.

37 Sturm, M., Holmgren, J., and Liston, G. E.: A seasonal snow cover classification system for local to  
38 global applications, *Journal of Climate*, 8, 1261-1283, 1995.

39 Sturm, M., Taras, B., Liston, G. E., Derksen, C., Jonas, T., and Lea, J.: Estimating snow water  
40 equivalent using snow depth data and climate classes, *Journal of Hydrometeorology*, 11, 1380-1394,  
41 2010.

42 Sturm, M.: White water: Fifty years of snow research in WRR and the outlook for the future, *Water*  
43 *Resources Research*, 51, 4948-4965, 10.1002/2015wr017242, 2015.

44 Takala, M., Luoju, K., Pulliainen, J., Derksen, C., Lemmetyinen, J., Kärnä, J.-P., Koskinen, J., and

1 Bojkov, B.: Estimating northern hemisphere snow water equivalent for climate research through  
2 assimilation of space-borne radiometer data and ground-based measurements, *Remote Sensing of*  
3 *Environment*, 115, 3517-3529, 2011.

4 Tedesco, M., Pulliainen, J., Takala, M., Hallikainen, M., and Pampaloni, P.: Artificial neural  
5 network-based techniques for the retrieval of SWE and snow depth from SSM/I data, *Remote sensing*  
6 *of Environment*, 90, 76-85, 2004.

7 Tedesco, M., and Narvekar, P. S.: Assessment of the NASA AMSR-E SWE Product, *IEEE Journal of*  
8 *Selected Topics in Applied Earth Observations and Remote Sensing*, 3, 141-159, 2010.

9 Tedesco, M., Derksen, C., Deems, J. S., and Foster, J. L.: Remote sensing of snow depth and snow  
10 water equivalent, *Remote Sensing of the Cryosphere*, 73-98, 2014.

11 Tedesco, M., and Jeyaratnam, J.: A New Operational Snow Retrieval Algorithm Applied to Historical  
12 AMSR-E Brightness Temperatures, *Remote Sensing*, 8, 2016.

13 Tennant, C. J., Harpold, A. A., Lohse, K. A., Godsey, S. E., Crosby, B. T., Larsen, L. G., Brooks, P. D.,  
14 Kirk, R. W. V., and Glenn, N. F.: Regional sensitivities of seasonal snowpack to elevation, aspect, and  
15 vegetation cover in western North America, *Water Resources Research*, 53, 2017.

16 Tilling, R. L., Ridout, A., Shepherd, A., and Wingham, D. J.: Increased Arctic sea ice volume after  
17 anomalously low melting in 2013, *Nature Geoscience*, 8, 643-646, 10.1038/ngeo2489, 2015.

18 Tsutsui, H., and Koike, T.: Development of Snow Retrieval Algorithm Using AMSR-E for the BJ  
19 Ground-Based Station on Seasonally Frozen Ground at Low Altitude on the Tibetan Plateau, *Journal of*  
20 *the Meteorological Society of Japan. Ser. II*, 90C, 99-112, 10.2151/jmsj.2012-C07, 2012.

21 Vander Jagt, B. J., Durand, M. T., Margulis, S. A., Kim, E. J., and Molotch, N. P.: The effect of spatial  
22 variability on the sensitivity of passive microwave measurements to snow water equivalent, *Remote*  
23 *Sensing of Environment*, 136, 163-179, 2013.

24 Wang, C., and Li, D.: Spatial-temporal variations of snow cover days and the maximum depth of snow  
25 cover in China during recent 50 years, *Journal of Glaciology and Geocryology*, 34, 247-256, 2012.

26 Wang, X., Xie, H., and Liang, T.: Evaluation of MODIS snow cover and cloud mask and its application  
27 in Northern Xinjiang, China, *Remote Sensing of Environment*, 112, 1497-1513,  
28 10.1016/j.rse.2007.05.016, 2008.

29 Wang, Y., Huang, X., Liang, H., Sun, Y., Feng, Q., and Liang, T.: Tracking Snow Variations in the  
30 Northern Hemisphere Using Multi-Source Remote Sensing Data (2000–2015), *Remote Sensing*, 10,  
31 10.3390/rs10010136, 2018.

32 Wegmann, M., Orsolini, Y., Dutra, E., Bulygina, O., Sterin, A., and Brönnimann, S.: Eurasian snow  
33 depth in long-term climate reanalyses, *The Cryosphere*, 11, 923-935, 10.5194/tc-11-923-2017, 2017.

34 Wentz, F. J.: SSM/I version-7 calibration report, *Remote Sensing Systems Tech. Rep.*, 11012, 46, 2013.

35 Wu, X., Che, T., Li, X., Wang, N., and Yang, X.: Slower Snowmelt in Spring Along With Climate  
36 Warming Across the Northern Hemisphere, *Geophysical Research Letters*, 45, 12,331-312,339,  
37 10.1029/2018gl079511, 2018.

38 Xiao, X., Zhang, T., Zhong, X., Shao, W., and Li, X.: Support vector regression snow-depth retrieval  
39 algorithm using passive microwave remote sensing data, *Remote Sensing of Environment*, 210, 48–64,  
40 2018.

41 Xu, X., Liu, X., Li, X., Xin, Q., Chen, Y., Shi, Q., and Ai, B.: Global snow cover estimation with  
42 Microwave Brightness Temperature measurements and one-class in situ observations, *Remote Sensing*  
43 *of Environment*, 182, 227-251, 2016.

44 Xue, Y., and Forman, B. A.: Comparison of passive microwave brightness temperature prediction

1 sensitivities over snow-covered land in North America using machine learning algorithms and the  
2 Advanced Microwave Scanning Radiometer, *Remote Sensing of Environment*, 170, 153-165, 2015.

3 Ye, H., Cho, H.-r., and Gustafson, P. E.: changes in russian winter snow accumulation during 1936-83  
4 and its spatial patterns, *Journal of Climate*, 11, 856-863, 1998.

5 Yu, H., Zhang, X., Liang, T., Xie, H., Wang, X., Feng, Q., and Chen, Q.: A new approach of dynamic  
6 monitoring of 5 - day snow cover extent and snow depth based on MODIS and AMSR - E data from  
7 Northern Xinjiang region, *Hydrological Processes*, 26, 3052-3061, 2012.

8 Zhang, T., Osterkamp, T., and Stamnes, K.: Influence of the depth hoar layer of the seasonal snow  
9 cover on the ground thermal regime, *Water Resources Research*, 32, 2075-2086, 1996.

10 Zhang, T.: Influence of the seasonal snow cover on the ground thermal regime: An overview, *Reviews*  
11 *of Geophysics*, 43, 589-590, 2005.

12 Zhang, Y., Li, T., and Wang, B.: Decadal Change of the Spring Snow Depth over the Tibetan Plateau\_  
13 The Associated Circulation and Influence on the East Asian Summer Monsoon, *Journal of Climate*, 17,  
14 2780-2793, 2004.

15 Zhong, X.: Spatiotemporal variability of snow cover and the relationship between snow and climate  
16 change across the Eurasian Contient, Lanzhou: Cold and Arid Regions Environmental and Engineering  
17 Research Institute, CAS, 2014.

18 Zhong, X., Zhang, T., and Wang, K.: Snow density climatology across the former USSR, *The*  
19 *Cryosphere*, 8, 785-799, 2014.

20 Zhong, X., Zhang, T., Kang, S., Wang, K., Zheng, L., Hu, Y., and Wang, H.: Spatiotemporal variability  
21 of snow depth across the Eurasian continent from 1966 to 2012, *The Cryosphere*, 12, 227-245,  
22 10.5194/tc-12-227-2018, 2018.

23

1 **List of Tables and Figures**

2 Table 1 Detail description for SSM/ and SSMIS sensors. H and V denotes horizontal and vertical  
 3 polarization, respectively.

Satellite	SSM/I		SSMIS
Platform	F 11	F 13	F 17
Temporal coverage	1991.12-1995.5	1995.5-2008.6	2006.12 -
Channels (GHz)	19 H, V; 22 V; 37 H, V; 85 H, V		19 H, V; 22 V; 37 H, V; 91 H, V

4

5 Table 2. Training sample filter rules

Layer ID	Filter rules
Layer2.	<p>If <math>\text{Number}_{total}(layer2) \leq 3000</math></p> <p style="text-align: center;"><math>\text{Number}_{training}(layer2) = (\text{Number}_{total}(layer2))/2</math></p> <p>Else <math>\text{Number}_{training}(layer2) = 3000</math></p>
Layer3.	<p>If <math>\text{Number}_{total}(layer3) \leq 3000</math></p> <p style="text-align: center;"><math>\text{Number}_{training}(layer3) = (\text{Number}_{total}(layer3))/2</math></p> <p>Else <math>\text{Number}_{training}(layer3) = 3000</math></p>
Layer1.	<p>If <math>\text{Number}_{training}(layer2) &gt; 2000</math> or <math>\text{Number}_{training}(layer3) &gt; 1000</math></p> <p style="text-align: center;"><math>\text{Number}_{training}(layer1)</math></p> <p style="text-align: center;"><math>= 15000 - \text{Number}_{training}(layer2) - \text{Number}_{training}(layer3)</math></p> <p>Else <math>\text{Number}_{training}(layer1) = 12000</math></p>

6

7 Table 3 Snow density estimation model parameters

Snow class	$\rho_{max}$	$\rho_0$	$k_1$	$k_2$	References
Alpine	0.5975	0.2237	0.0012	0.0038	Sturm et al. (2010)
Maritime	0.5979	0.2578	0.0010	0.0038	
Prairie	0.5940	0.2332	0.0016	0.0031	
Tundra	0.3630	0.2425	0.0029	0.0049	
Taiga	0.2170	0.2170	0	0	
Ephemeral	0.2500	0.2500	0	0	Zhong et al. (2014)

8

1 Table 4. The evaluated indexes (bias, MAE, RMSE; unit: cm) for three gridded SD products (NHSnow,  
2 GlobSnow, ERA-Interim/Land).

Products	Bias	MAE	RMSE
NHSnow	0.59	15.12	20.11
GlobSnow	1.19	15.98	15.48
ERA-Interim/Land	-5.60	18.72	37.77

3

4 Table 5. Rules of variation level grading

Variation rate	P value	Variation level
rate < 0	$p \leq 0.01$	extremely significant decrease
rate < 0	$0.01 < p \leq 0.05$	significant decrease
-	$P > 0.05$	non-significant change
rate $\rightarrow$ 0	$0.01 < p \leq 0.05$	significant increase
rate $\rightarrow$ 0	$p \leq 0.01$	extremely significant increase

5

6 Table 6. Mean variation rate of average SD (cm yr.<sup>-1</sup>) over the Northern Hemisphere for three common  
7 period (1992-2016, 1992-2001, 2002-1996) and snow cover seasons (fall, winter, spring). Std. means  
8 standard deviation

Season	1992-2016 (Mean $\pm$ 1 Std.)	1992-2001 (Mean $\pm$ 1 Std.)	2002-2016 (Mean $\pm$ 1 Std.)
Fall	-0.08 $\pm$ 0.11	-0.01 $\pm$ 0.19	-0.15 $\pm$ 0.22
Winter	-0.11 $\pm$ 0.40	0.06 $\pm$ 0.62	-0.22 $\pm$ 0.75
Spring	-0.04 $\pm$ 0.25	0.02 $\pm$ 0.51	-0.07 $\pm$ 0.41
Year	-0.06 $\pm$ 0.20	0.02 $\pm$ 0.35	-0.11 $\pm$ 0.34

9

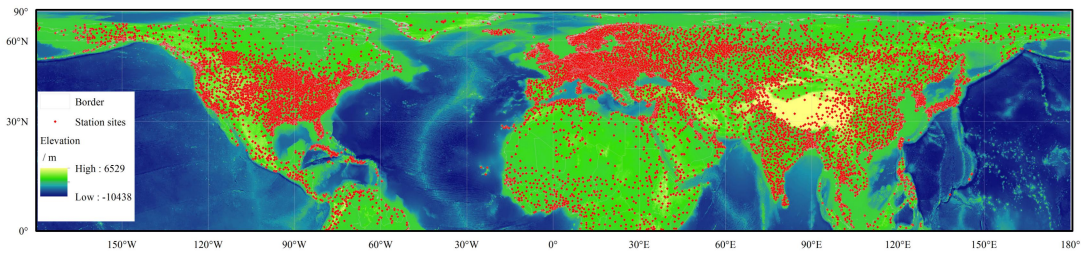
10 Table 7. Variation rate and changes of monthly average snow mass during 1992-2016. The asterisk  
11 indicate that the changes are significant at 95% confidence level

Month	Variation rate (km <sup>3</sup> /yr.)	% Change in the mean of monthly average snow mass
September	-5.96*	-63.89%

October	-25.50*	-43.99%
November	-36.50*	-26.96%
December	-32.66*	-5.00%
January	-34.38*	-9.53%
February	-30.89*	-11.91%
March	1.90	-4.30%
April	-4.29	-6.46%
May	-11.33*	-19.59%
June	-8.01*	-64.67%

1

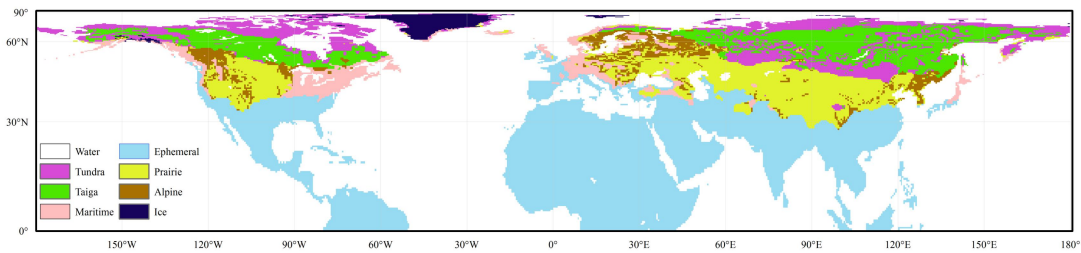
2



3

Figure 1. Distribution of Meteorological stations overlaid on ETOPO1 in the Northern Hemisphere.

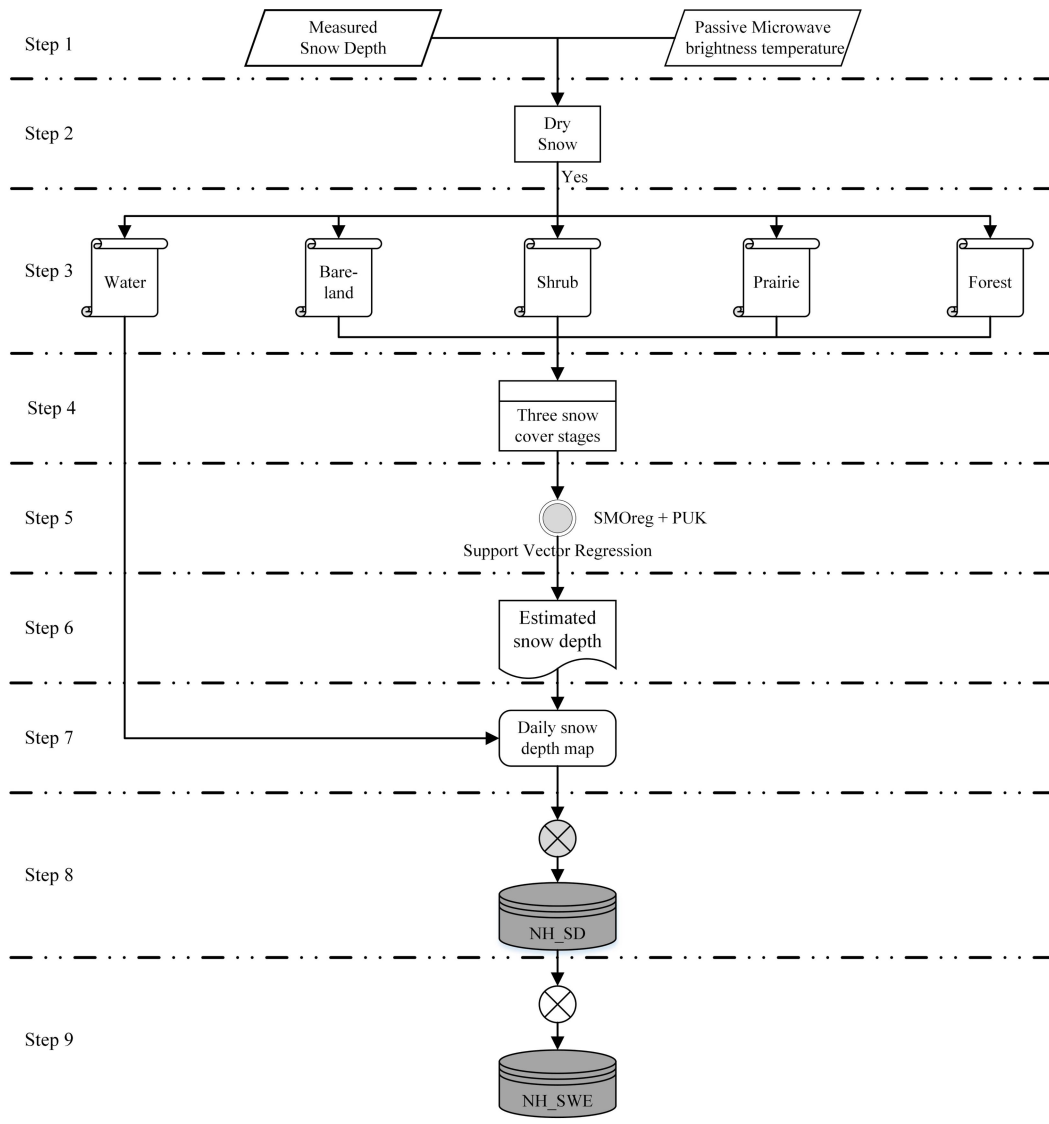
5



6

7

Figure 2. Snow Class distribution in the Northern Hemisphere



1  
2  
3  
4  
5

Figure 3. Process flowchart diagram for developing Northern Hemisphere daily snow depth and snow water equivalent data

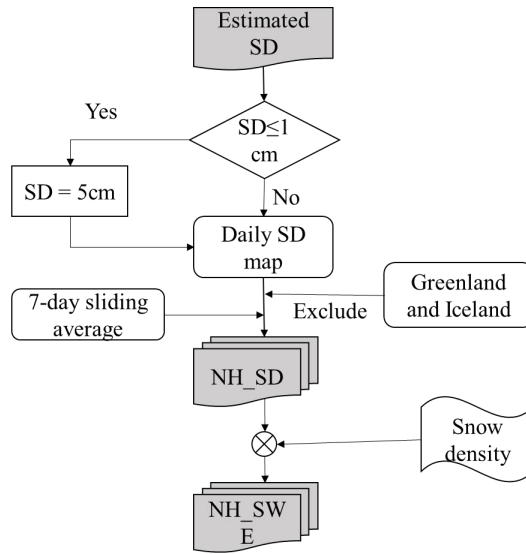


Figure 4. Flowchart diagram of the generation of NHSnow products.

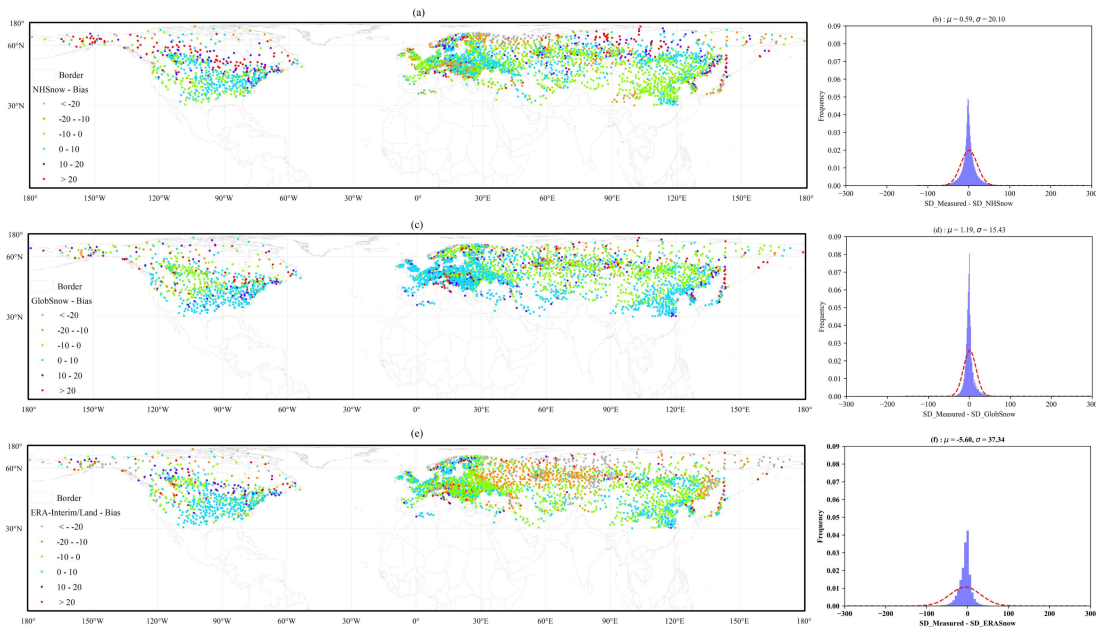
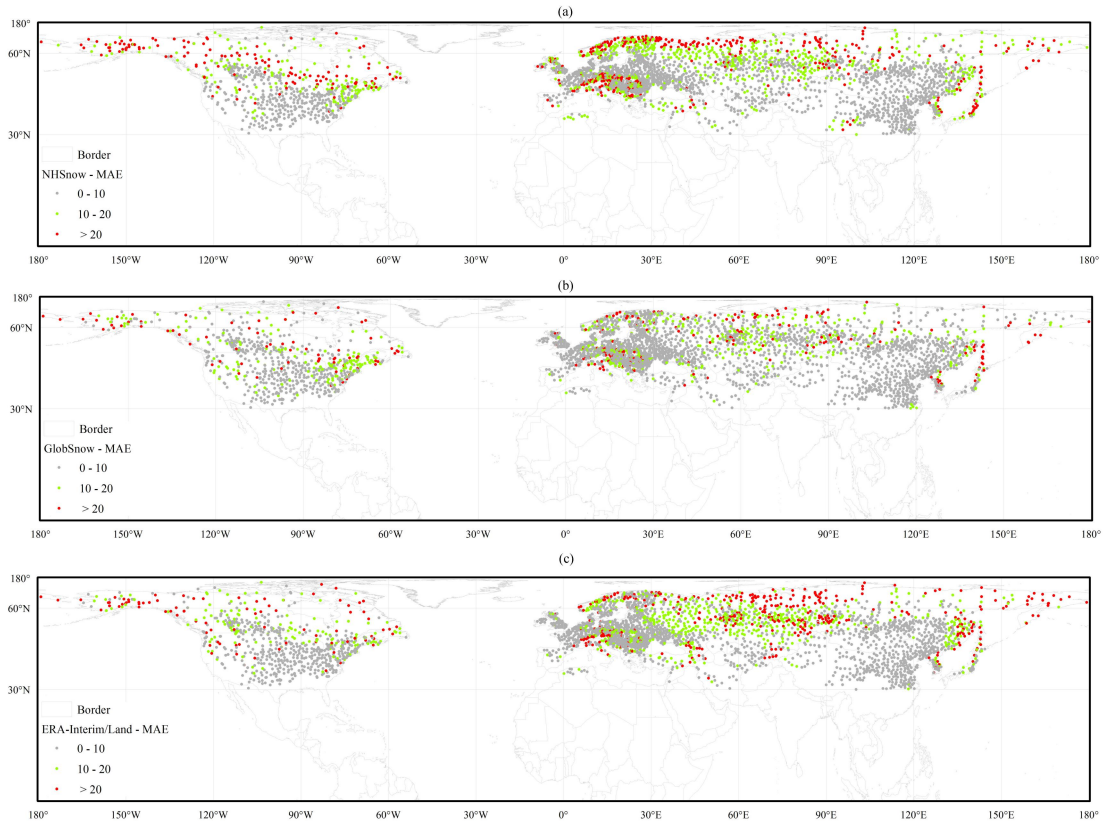
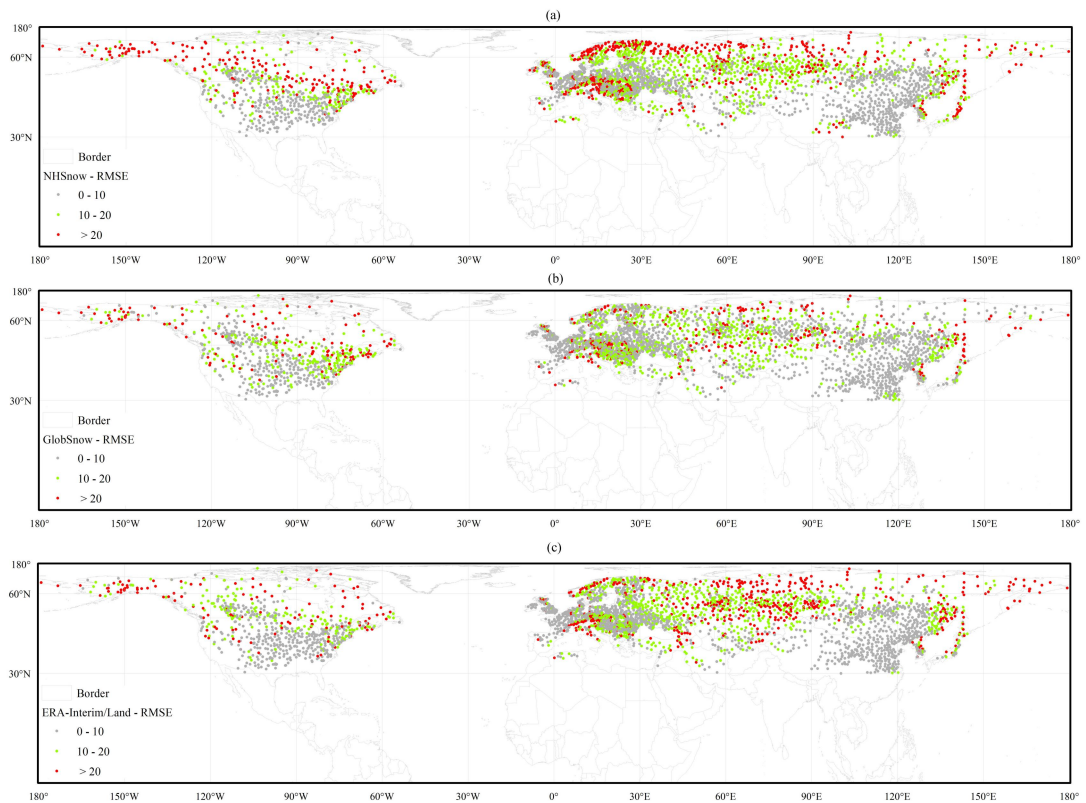


Figure 5. Bias of each meteorological station and histogram of biases for three products: a), b) NHSnow; c), d) GlobSnow, e), f) ERA-Interim/Land. The red dashed line in right column figures are the fitted normal distribution curve



1  
2 Figure 6. MAE of each meteorological station for three products: a) NHSnow, b) GlobSnow, c)  
3 ERA-Interim/Land.

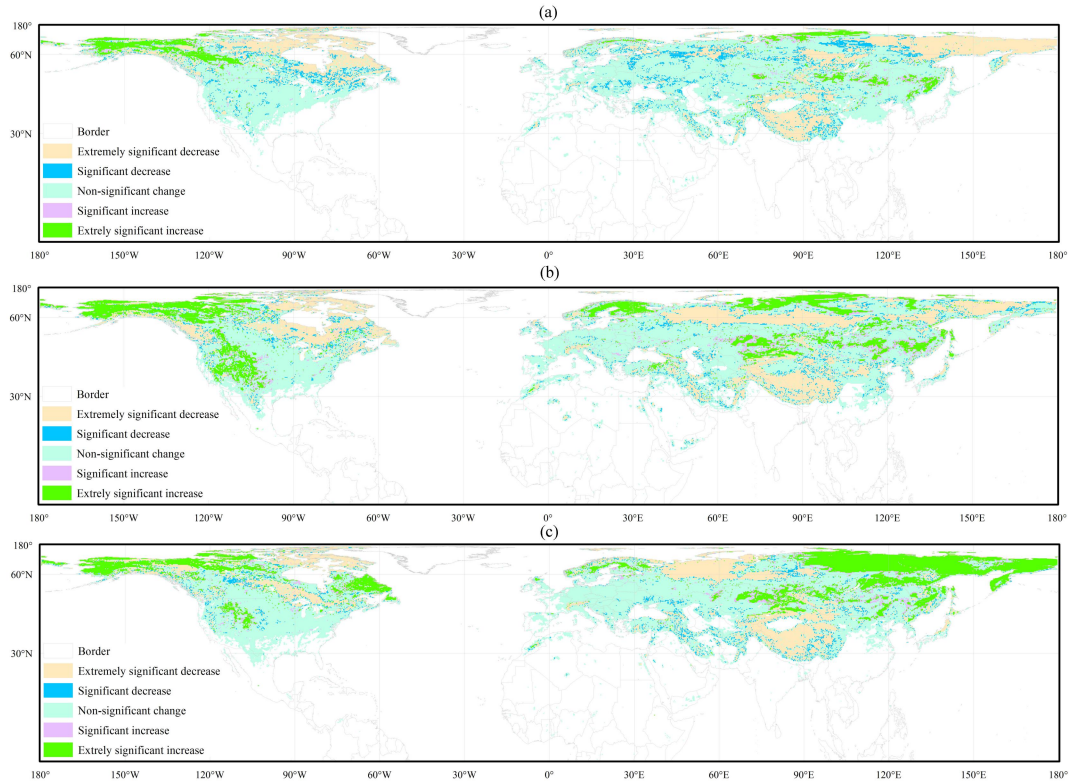


4  
5 Figure 7. RMSE of each meteorological station for three products: a) NHSnow, b) GlobSnow, c)

1

ERA-Interim/Land.

2



3

4

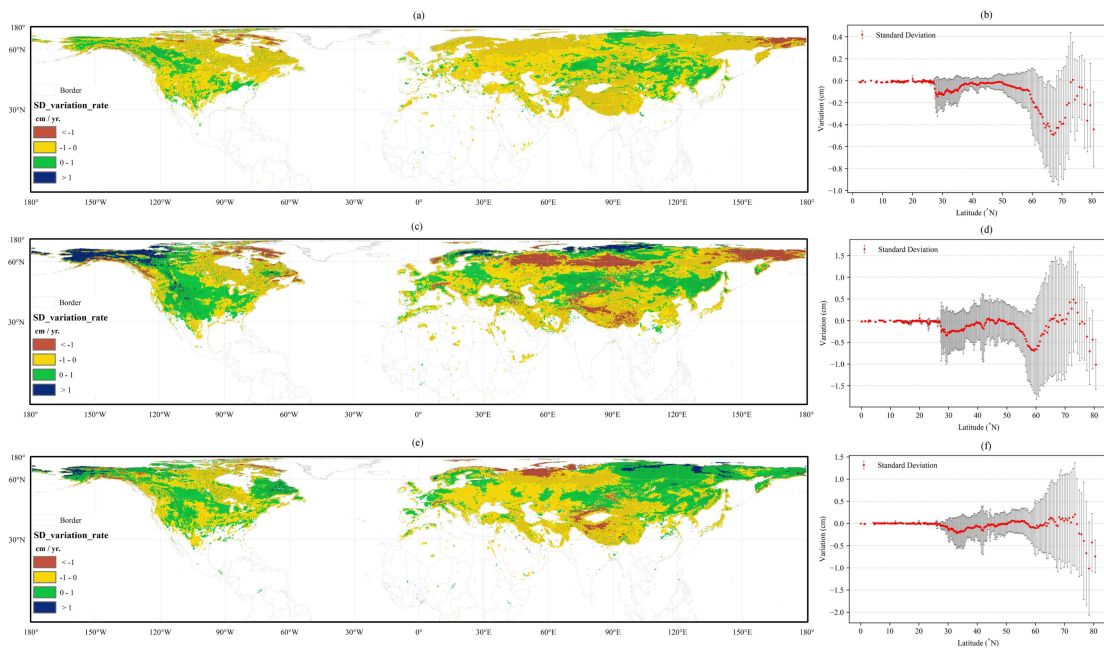
Figure 8. The variation rate pattern of season maximum SD with statistical significances over the

5

Northern Hemisphere for three snow cover season, fall (a; September to November), winter (b;

6

December to February), spring (c; March to June) from 1992-2016.



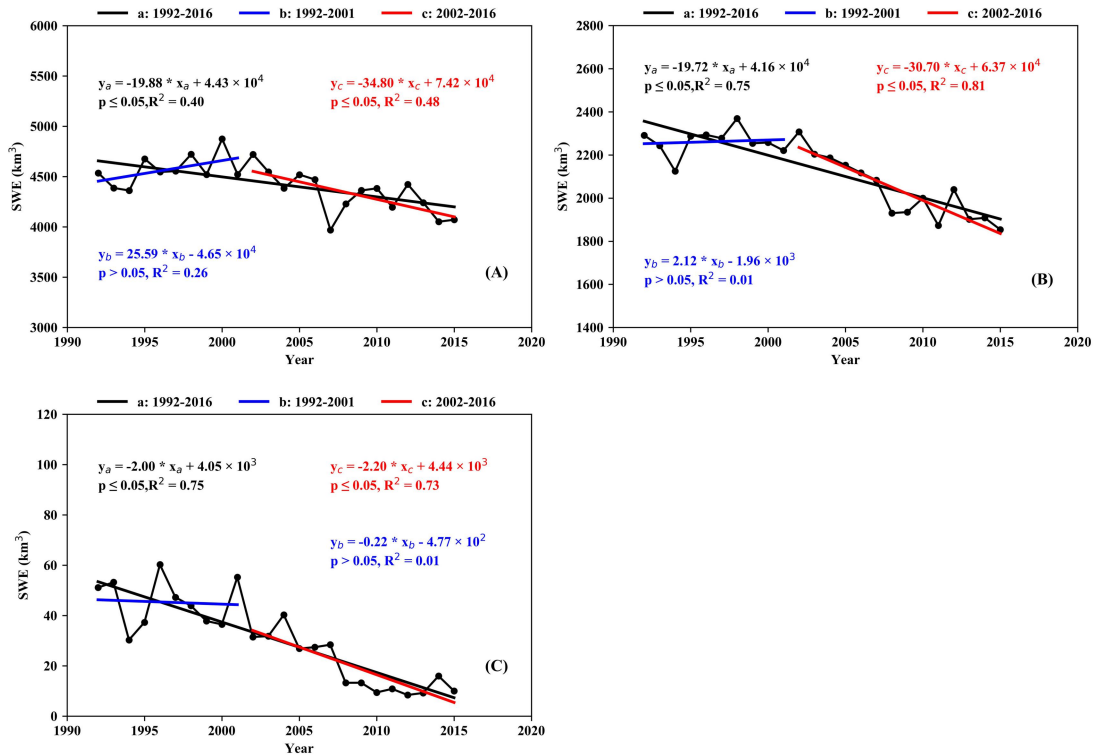
7

8

Figure 9. The variation rate pattern of season average SD over the Northern Hemisphere for three snow

1 cover season, fall (a, b; September to November), winter (c, d; December to February), spring (e, f;  
 2 March to June) from 1992-2016. Black dots in (a, c, e) indicate that the changes are significant at 95%  
 3 confidence level (CL). The zonal distribution in (b, d, f) are mapped at 0.25 degree resolution in  
 4 latitude. The error bars in (b, d, f) is one times of standard deviation.

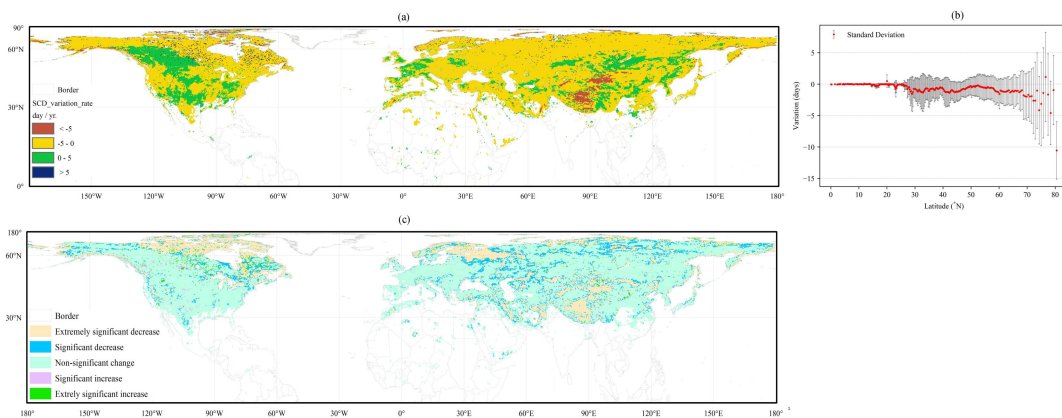
5



6

7 Figure 10. Interannual variation of annual maximum snow mass (A), annual average snow mass (B)  
 8 and annual minimum snow mass (C) over the Northern Hemisphere for three period 1992-2016 (black  
 9 line), 1992-2001 (blue line), and 2002-2016 (red line). Trends estimates were computed from least  
 10 squares. P is the confidence level for the coefficient estimates;  $R^2$  is the goodness of fit coefficient.

11



12 Figure 11. The variation rate pattern of SCD (a) and their statistical significances (c) over the Northern

- 1 Hemisphere from 1992-2016. The zonal distribution in (b) are mapped at 0.25 degree resolution in
- 2 latitude. The error bars in (b) is one times of standard deviation.
- 3